Robust Planning of Distributed Battery Energy Storage Systems in Flexible Smart Distribution Networks: A Comprehensive Study

Seyed Aboozar Bozorgavari[1], Jamshid Aghaei[1,2], Sasan Pirouzi[3], Ahmad Nikoobakht[4]

Hossein Farahmand[2], and Magnus Korpås[2]

[1]Department of Electrical and Electronics Engineering, Shiraz University of Technology, Shiraz, Iran

[2]Department of Electric Power Engineering, Norwegian University of Science and Technology (NTNU), Trondheim NO-7491, Norway

[3]Faculty of Engineering, Semirom Branch, Islamic Azad University, Semirom, Esfahan, Iran

[4]Higher Education Center of Eghlid, Eghlid, Iran

[*]Corresponding Author: **J. Aghaei**, e-mail: aghaei@sutech.ac.ir

Abstract- This paper presents a robust planning of distributed battery energy storage systems (DBESSs) from the viewpoint of distribution system operator (DSO) to increase the network flexibility. Initially, the deterministic model of the proposed problem is expressed by minimizing the difference between the DBESS planning, degradation and operation (charging) costs and the revenue of DBESS from selling its stored energy subject to the constraints of AC power flow equations in the presence of RESs and DBESSs, and technical limits of the network indexes, variable renewable energy sources (vRESs) and DBESSs. This problem is modeled as a non-linear programming (NLP), then, an equivalent linear programming (LP) model is proposed using the first-order expansion of Taylor's series for linearization of power flow equations and a polygon for linearization of circular inequalities. Also, to model the uncertain parameters in the proposed problem including forecasted active and reactive loads, energy and charging/discharging prices and the output power of vRES, the bounded uncertainty-based robust optimization (BURO) framework is proposed in the next step. Finally, the proposed scheme is applied to 19-bus MV CIGRE benchmark grid by GAMS software to investigate the capability and efficiency of the model.

Highlights

- Investment planning of distributed battery energy storage systems is modeled.
- The planning problem is modeled linearly from DSO viewpoint.

- Simple degradation cost of batteries is considered in the optimization.
- Robust optimization is implemented to handle the uncertainty of PVs.

Keywords: Bounded Uncertainty-Based Robust Optimization, Distributed Battery Energy Storage Systems, Distribution System Operator, Robust Planning, Variable Renewable Energy Sources, Smart Distribution Network, System Flexibility.

NOMENCLATURE

1) *Acronyms*

ABC	Artificial bee colony
BD	Benders decomposition
BESS	Battery energy storage systems
BURO	Bounded uncertainty-based robust optimization
DBESS	Distributed battery energy storage system
DE	Differential evolution
DOD	Depth Of Discharge
DSO	Distribution system operator
ESS	Energy storage system
FBS	Forward-backward sweep
HESS	Hybrid energy storage system
LP	Linear programming
LT	Lithuania
LV	Low voltage
MILP	mixed integer linear programming
MSC	Maximum storage capacity
NLP	Non-linear programming
OPF	Optimal power flow
PDF	Probability density function
PV	Photovoltaic

RO	Robust optimization
ROSION	Robust Optimization of Storage Investment On Networks
SOC	State of charge
SOCP	Second order cone programing
vRES	Variable renewable energy sources

2) *Indices and Sets*

(b,j), t, l, k, p	Indices of bus, time, linearization segments of voltage magnitude term, circular constraint and term of degradation of battery, respectively
φ_b, φ_t, φ_l, φ_k, φ_p	Sets of bus, time, linearization segments of voltage magnitude term, circular constraint and term of degradation of battery, respectively
m, n_f	Index and total number of iteration for the primal sub-problem to be feasible, respectively
r, n_i	Index and total number of iteration for the primal sub-problem to be infeasible, respectively

3) *Parameters*

A	Bus incidence matrix (if line exists between buses b and j, $A_{b,j}$ is equal to 1, and 0 otherwise)
A_{min}	Minimum boundary rate of the stored energy in battery
c^s	Annual investment cost (in \$/MWh/year)
g, b	Line conductance and susceptance in per unit (pu), respectively
$P^{ch\text{-}max}$, $P^{dis\text{-}max}$	Maximum charging and discharging rate of battery in pu, respectively
PD, QD	Active and reactive load in pu, respectively
$VRES$	The output power of vRES in pu
SS^{max}, SL^{max}	Maximum loading of distribution line and station in pu, respectively
T	Operating horizon, i.e., 6, 12, 24 or 48 hours
V^{max}, V^{min}, ΔV^{max}	Maximum and minimum voltage magnitude, and maximum value of voltage deviation in pu, respectively
V_{ref}	Voltage of reference (distribution station) bus in pu
X, Y	Horizontal and vertical value of different points of cycle life loss curve, respectively
ω_{max}	Maximum capacity of battery in pu

η_{ch}, η_{dis}	Efficiency of charging and discharging of the battery, respectively
λ^{ch}, λ^{dis}	Charging and discharging price of the battery, respectively in \$/MWh

4) *Variables*: All variables are in per unit (pu)

D	Depth of discharge without unit
E	Stored energy of battery
P^{ch}, P^{dis}	Amount of electricity charged and discharged from battery
PS, QS	Active and reactive power of the distribution station, respectively
PL, QL	Active and reactive power of lines, respectively
V, ΔV, θ	Magnitude, deviation (pu) and angle of voltage (in rad), respectively
ω	Capacity of battery
λ_{sub}, μ_{sub}	Dual variables of equality and inequality constraints in the primal sub-problem
ρ, γ	Cycle life loss and auxiliary variable for storage degradation cost, respectively

5) *Functions*

f	Cycle life loss
J_p, J_{sub}	Master problem and sub-problem objective functions in pu
β_1	Operation or charging cost of DBESS in pu
β_2	Revenue of DBESSs for selling discharging power in pu

1. Introduction

Uncertain variable renewable energy sources (vRESs) in electricity networks experience a substantial growth due to cost reductions, technology improvements, climate change awareness and different support schemes. RESs variable generation along with customers' emerging proactive role in power system operation, and their expanding technology options such as solar photovoltaics panels, deployment of plug-in electric vehicles and smart appliances, drive the need for higher power system flexibility. Although different definitions for flexibility have been proposed, one of them is more used by system operators which defines flexibility as "*the modification of generation injection and/or consumption patterns in reaction to an external price or activation signal in order to provide a service within the electrical system*" [1]. Flexibility can be provided by supply side, network side, and demand side and energy storage systems. Some important flexible resources are demand response programs, distributed battery energy storage systems and non-renewable distributed energy sources, e.g., micro-turbines and fuel cells, in the demand and smart distribution network sides. Among these flexible resources, batteries are capable of providing high flexibility due to their inherent fast dynamics combined with fast control based on the power electronic converters [2]. However, allocating more distributed battery energy storage systems (DBESSs) to the smart distribution networks imposes extra costs, accordingly, it is crucial to establish investment planning models to determine how much flexibility from DBESSs might be needed and of where to place them in the network. Finding the optimal investment level requires consideration not only of short-term power system operation procedures, but also long-term investment planning to recover costs. Moreover, the flexibility of DBESSs and their associated costs are system-dependent. Accordingly, it is essential to develop methodologies and procedures to measure economic and technical flexibility benefits of DBESSs and their potential capacity to host adequate vRES, e.g., photovoltaic (PV) systems and wind power generation. In other words, it is necessary to make compromises between upgrading the system flexibility levels of DBESSs and avoiding extra investment in supply and grid reinforcements. In this regard, the concentration areas of this work are to answer two main questions: "*How does integrating vRES affect the power system operation and planning procedures?*" and "*How to allocate DBESSs as the flexibility resources to accommodate a higher penetration of vRES in the distribution grids?*". To this end, the first step is to determine the optimal location and size of batteries in the distribution networks planning studies [2]. However, the battery planning problem generally is a probabilistic or stochastic optimization problem due to the presence of uncertain parameters. This calls for some scenario-based stochastic programming modeling of uncertain parameters that assumes there is a probabilistic description of the uncertainty based on probability density functions (PDFs). Generally, the scenario-based stochastic modeling of planning problem enforces the high computational burden and calculation time and increase the complexity of the optimization solution methodology. Robust optimization (RO) is an alternative approach for modeling uncertainty in optimization problems that works with a deterministic, set-based description of the uncertainty to construct a solution that is feasible for any realization of the uncertainty in a given set [3].

Significant research works have been concentrated on the planning of battery energy storage systems (BESSs) requirement as well as evaluating their effects in the power system operation in the presence of vRES. For instance, the different technologies of energy storage system (EES) and various methods for combination of ESS and vRES are presented in [4-8] for a zone to improve the system flexibility and reduce variability of RES. In [4], the hybrid

ESS and power electronic devices is introduced. Also, the combination of ESS and wind system is used in [5] and [6] and this method is used in [7] for combination of different vRESs and ESSs. Moreover, the authors of [8] have presented a comprehensive review of ESS technologies that are currently engaged for power applications such as pumped hydro, compressed-air, battery, flywheel, capacitor and etc. Then, the study compares the characteristics of these systems, and presents their technological development status and capital costs.

In addition, a two-stage stochastic optimization problem of integrated investment planning of PVs, BESS and gas-fired micro turbines has been proposed in a multicarrier gas and electricity system in [9]. The first stage of the proposed framework in [9] deals with the optimal investment planning of the ESSs to decide their size and location. Then, according to the results of the first stage, the optimal operation is executed based on the power flow equations in both gas and electricity grids. Different operational considerations of integrating PVs in the low voltage distribution networks have been addressed in [10] including the changes in the voltage profile, reverse power flow, and energy losses. Also, in [10], a localized BESS has been suggested as a possible solution to improve the system operation conditions in the presence of high penetration of PVs. For this purpose, the battery is charged when PV production is more than consumers' demands and discharged when consumers' demands are increased. It is noted that while the investment costs of batteries are high, hence using an objective function based on both economic and environmental goals is important for the placement and sizing of batteries. In addition to the above researches, the optimal sizing of a hybrid PV and battery storage system has been studied from prosumer viewpoint for residential and nonresidential customers in [11]. To determine the optimal sizing and location of battery systems connected to the distribution grids based on AC power flow equations, an optimal planning scheme has been presented in [12] wherein a relaxation method based on the second order cone programing (SOCP) of the optimal power flow (OPF) algorithm has been implemented. Also, a relaxation method for the OPF has been used in [13] to decide on the optimal placement and sizing of BESSs while considering the uncertain natures of the customers' demands and vRES generations. In addition, the authors of [14] have used the multi-objective and three-level model based on AC power flow equations for expansion planning of active distribution networks and storage systems as well as vRES, simultaneously. Also, the optimal size of ESS based on the state of energy model has been addressed in [15] for the active distribution networks, and the optimal siting and sizing of ESS has been modeled in [16] for this network considering reconfiguration technique. Moreover, the storage planning model is used in [17] for distribution networks considering wind systems based of the NLP formulation.

From the perspective of the optimization solution methodology for battery storage planning, different approaches have been conducted in the available researches in the area. For instance, the evolutionary algorithms such as differential evolution (DE) algorithm [18], artificial bee colony (ABC) algorithm [19] have been used for the storage system planning based on AC OPF equations. Also, in [20]-[21], the storage planning is presented based on Benders decomposition (BD) approach wherein the master problem and sub-problem of this scheme, respectively considers the storage planning and the OPF both on the electricity markets [20] and medium voltage (MV) distribution networks [21]. Both the proposed BD approaches in [20] and [21], are in the form of mixed integer linear programming (MILP) modeling for a DC OPF and a simple linearized forward-backward sweep (FBS) AC OPF formulations, respectively.

Furthermore, to deal with the uncertainty modeling in the storage planning problems, different frameworks have been employed. Robust OPF formulations for distribution networks using non-linear adaptive RO and linear bounded uncertainty-based RO have been expressed in [22] and [23], respectively. The proposed non-linear RO in [18] has a complex formulation of the duality gap and complementarity (equilibrium) constraints. However, the linear RO in [23] benefits from a simple formulation and a low calculation time. The robust operation problem for ESSs considering the uncertainty of load profiles has been presented in [24]. In [25], a developed optimization tool, termed Robust Optimization of Storage Investment on Networks (ROSION), employs the RO to minimize the investment in the storage units that guarantees feasible system operation without load or renewable power curtailment for all scenarios in the convex hull of a discrete uncertainty set.

To have an overall view on the available researches in the subject of energy storage planning problem, the taxonomy of recent works in the area is listed in Table I.

Table I: Taxonomy of recent works in the area

Ref. No.	Flexibility	Robust model	Improvement of the network indexes	Power Flow		Problem model	Solution method
				AC	DC		
[4]-[8]	Combination of ESS and vRES are considered to reduce variability of RES and improve the flexibility in a zone						
[9]-[11]	No	No	Yes	No	Yes	LP	Simplex method
[12]-[13]	No	No	Yes	Yes	No	LP	Relaxation method
[14]-[19]	No	No	Yes	Yes	No	NLP	Evolutionary algorithms
[20]	No	No	Yes	No	Yes	MILP	Benders decomposition
[21]	No	No	Yes	Yes	No	MILP	Benders decomposition
[24]	No	Yes	Yes	No	Yes	LP	Simplex method
[25]	No	Yes	Yes	No	Yes	MILP	Simplex method
Proposed	**Yes**	**Yes**	**Yes**	**Yes**	**No**	**LP based on BD**	**Benders decomposition**

method	approach

As inferred from Table I, there are different main research gaps for available literature about storage system planning as follows:

- Different researches such as [4-8] express that RES should be combined with ESS to reduce its variability considering centralized ESS approach. Nevertheless, it is anticipated that this method is costly, especially, if the large size used to RES, and it cannot significantly enhance the network indices. Therefore, the distributed ESS approach that decides the ESSs size and location for different zones of the network can achieve better values for the network indices with respect to the centralized ESS approach .
- In some researches, the planning problem of the storage system is based on the DC OPF [9]-[11] and [20]. However, the DC OPF is not suitable for the distribution networks since it ignores the power losses and reactive power. Accordingly, the AC OPF has been adopted in [12]-[19] and [21], where [12]-[13] and [14]-[19] are using a relaxation method and evolutionary algorithms, respectively. Nevertheless, these methods are based on the random search iteration methods which are not suitable for the robust modeling. Furthermore, as above mentioned, the simplified linear AC OPF suggested in [21] employs the FBS OPF formulation which fits to the structure of the radial distribution networks rather than the bidirectional flow ones.
- The robust operation of the distribution networks has been adopted in [22]-[24]. Also, the uncertainty modeling of the vRES has been directed using the robust planning of storage systems in [25].

As a complimentary work to the above researches, this paper develops a robust planning of DBESSs from the viewpoint of DSOs to increase the network flexibility. In the first step, a deterministic model of the proposed storage planning problem is formulated based on the structure of distribution grids illustrated in Fig. 1. In this step, the difference between the DBESS planning, degradation and operation (charging) costs and revenue of DBESS owing to selling its stored energy to the network is minimized as an objective function subject to the constraints of AC OPF in the presence of vRES and DBESSs, and technical limits of the network. As shown in Fig. 1 (a), the main assumptions of the proposed storage planning problem are as follows:

– The network includes different kinds of prosumers with the integrated vRES, e.g., PV systems, as well as flexible and inflexible loads.

– Each bus is a candidate to install battery as shown in Fig. 1(a).

Furthermore, the optimal sizing and siting of the DBESSs require the resolution of a temporal and spatial problem based on Fig. 1(b). The temporal problem involves integrated sequential time intervals to ensure consistency of the battery state of charge (SOC) between different consecutive time intervals, here it is assumed to be one hour for the DBESS planning problem. Therefore, the proposed problem is modeled as a non-convex NLP form that is not suitable for the robust optimization model owing to the high calculation time. Consequently, this paper suggests an equivalent LP model based on the BD approach by means of the first-order expansion of Taylor's series to linearize power flow equations and develop a polygon for linearization of circular inequalities of the problem. Moreover, to model the uncertainties of active and reactive loads, energy or charging/discharging prices and output power of vRES, a bounded uncertainty-based robust optimization (BURO) framework is proposed. Briefly, the main contributions of this paper with respect to the previous works in the area are summarized as follows:

- Developing a computationally-efficient optimization model for the investment planning of DBESSs in the distribution networks as a LP form based on the BD approach.
- Presenting a robust model based on BURO framework for DBESS planning on account of different uncertainties.

The rest of the paper is organized as follows: Section 2 describes the deterministic model of DBESS planning, and Section 3 presents the robust model and solution methodology based on the BD approach. Sections 4 and 5 address numerical simulations and the main conclusions of the paper, respectively.

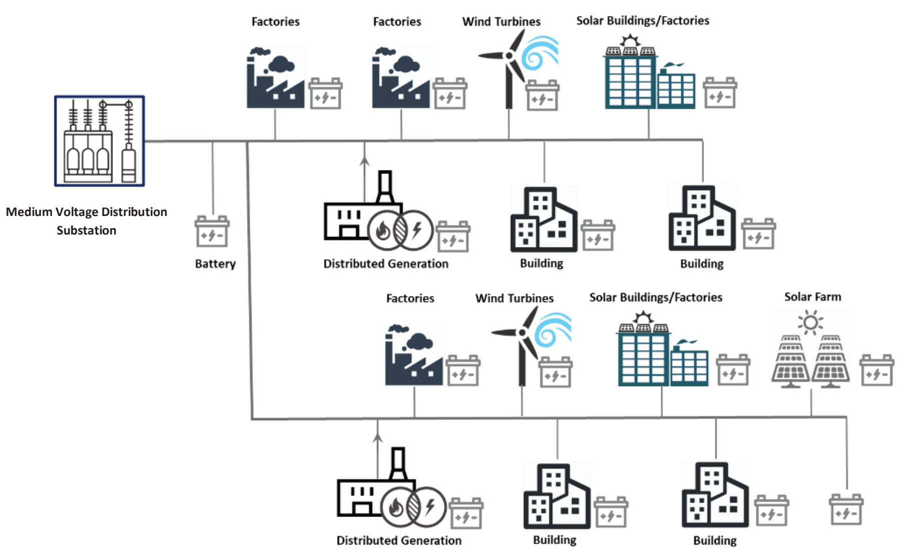

(a)

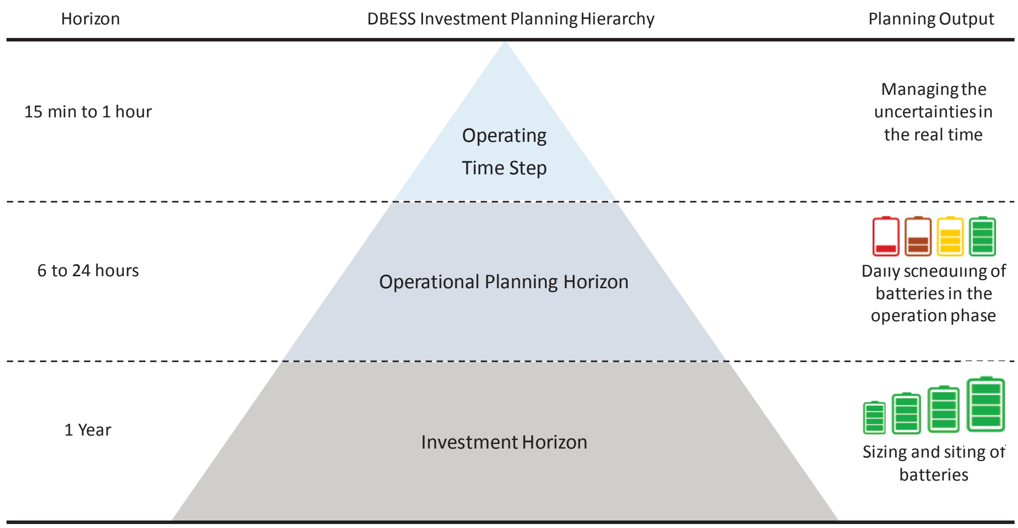

(b)

Fig. 1: (a) Medium voltage (MV) grid, (b) different time horizons in planning model of battery sizing and siting.

2. Deterministic Placement and Sizing of DBESS

2.1. Original NLP Model

In this section, the modeling of the optimal placement and sizing of DBESS is presented. The objective function of the investment planning of DBSS optimization problem is to minimize the difference between the DBESS annual cost and revenue as shown in (1a). The DBESS cost includes the investment, degradation and operation terms, and DBESS revenue is equal to the selling of battery stored energy (discharging) to the network. In addition, the proposed optimization problem is constrained by AC power flow equations, network operation limits and operation and planning equations of DBESSs. Accordingly, the proposed original non-linear model for one year time horizon to one hour time step can be written as follows:

$$J=\min \overbrace{\sum_{b\in\varphi_b} c_b^s.\omega_b}^{\textit{Annual investment cost}} + \overbrace{\sum_{t\in\varphi_t}\sum_{b\in\varphi_b} c_b^s.\omega_b.\max\left(f_b\left(D_{b,t}\right)-f_b\left(D_{b,t-1}\right),0\right)}^{\textit{Annual degradation cost of storage}} + \overbrace{\sum_{t\in\varphi_t}\sum_{b\in\varphi_b}\lambda_t^{ch}P_{b,t}^{ch}}^{\textit{Annual operational cost of storage}} - \overbrace{\sum_{t\in\varphi_t}\sum_{b\in\varphi_b}\lambda_t^{dis}P_{b,t}^{dis}}^{\textit{Annual revenue of storage}} \tag{1a}$$

S.to:

$$PS_{b,t}-\sum_{j\in\varphi_b}A_{b,j}PL_{b,j,t}+\left(P_{b,t}^{dis}-P_{b,t}^{ch}\right)=PD_{b,t}-VRES_{b,t} \quad \forall\, b,t \tag{1b}$$

$$QS_{b,t}-\sum_{j\in\varphi_b}A_{b,j}QL_{b,j,t}=QD_{b,t} \quad \forall\, b,t \tag{1c}$$

$$PL_{b,j,t} = g_{b,j}\left(V_{b,t}\right)^2 - V_{b,t}V_{j,t}\left(g_{b,j}\cos\left(\theta_{b,t}-\theta_{j,t}\right)+b_{b,j}\sin\left(\theta_{b,t}-\theta_{j,t}\right)\right) \quad \forall b,j,t \tag{1d}$$

$$QL_{b,j,t} = -b_{b,j}(V_{b,t})^2 + V_{b,t}V_{j,t}\left(b_{b,j}\cos\left(\theta_{b,t}-\theta_{j,t}\right)-g_{b,j}\sin\left(\theta_{b,t}-\theta_{j,t}\right)\right) \quad \forall b,j,t \tag{1e}$$

$$\theta_{b,t} = 0 \quad \forall\, b = reference\ bus, t \tag{1f}$$

$$\left(PL_{b,j,t}\right)^2 + \left(QL_{b,j,t}\right)^2 \le \left(SL_{b,j}^{\max}\right)^2 \quad \forall\, b,j,t \tag{1g}$$

$$\left(PS_{b,t}\right)^2 + \left(QS_{b,t}\right)^2 \le \left(SS_b^{\max}\right)^2 \quad \forall\, b,t \tag{1h}$$

$$V^{\min} \le V_{b,t} \le V^{\max} \quad \forall\, b,t \tag{1i}$$

$$E_{b,t} = E_{b,t-1} + \eta_{ch}P_{b,t}^{ch} - \frac{1}{\eta_{dis}}P_{b,t}^{dis} \quad \forall\, b,t \tag{1j}$$

$$0 \le P_{b,t}^{ch} \le P_b^{ch-\max} \quad \forall\, b,t \tag{1k}$$

$$0 \le P_{b,t}^{ch} \le P_b^{dis-\max} \quad \forall\, b,t \tag{1l}$$

$$A_{\min}\omega_b \le E_{b,t} \le \omega_b \quad \forall\, b,t \tag{1m}$$

$$E_{b,0} = E_{b,T} \quad \forall\, b \tag{1n}$$

$$D_{b,t} = \left(1 - \frac{E_{b,t}}{\omega_b}\right) \quad \forall\, b,t \tag{1o}$$

$$0 \le \omega_b \le \omega_{\max} \qquad \forall b \tag{1p}$$

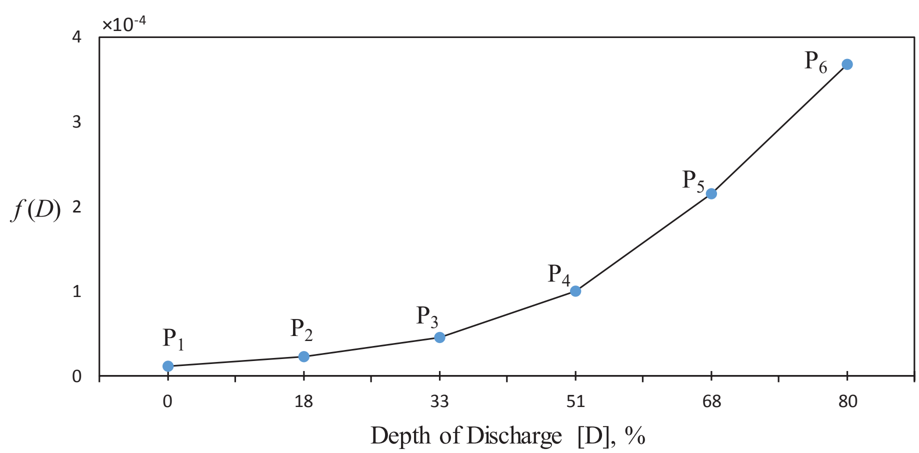

Fig. 2: Cycle life loss as a function of the DOD [26]

The objective function (1a) is equal to the difference between the sum of annual investment, degradation and operation cost of the storage systems and their annual revenue. It is noted that the term f in the degradation cost equation is cycle life loss that is equal to the inverse of cycle life of battery, and it depends on depth-of-discharge (DOD) as shown in Fig. 2 [26], and $f(D_{t-1})$ is zero at $t = 1$. Also, the cycle life states the number of cycles, each to the specified discharge and charge termination criteria under a specified charge and discharge regime that a battery can experience before deteriorating its specified nominal life criteria [2].

The AC power flow equations are denoted by (1b) to (1f) [27]-[29], where these equations represent the active power balance, reactive power balance, active power flow of lines, reactive power flow of lines and the value of the reference bus voltage angle, respectively. It is noted that the output power of vRES is modeled as a constant, hence, it is considered as a PQ bus, i.e., their active and reactive powers are pre-specified in different nodes. Also, the terms *PS* and *QS* are used for the distribution station that is connected to the reference bus. Thus, these terms are zero for the other buses. The network operation limits are represented in (1g) to (1i) [29] that are limits of bus voltage, line power flow, and substation power, respectively. In addition, the temporal constraints of the operating batteries are addressed in (1j) to (1o) and the constraints of batteries planning are shown in (1p) [21]. The stored energy of the battery in period t depends on the stored energy in the previous period, and charging or discharging in the current period. These impacts are replicated by (1j). The charging, discharging, and the stored energy must be within the minimum and maximum limits as expressed in (1k) to (1m). An additional constraint is added to avoid yearly accumulation effects by forcing the stored energy of the first and last time interval of the operating time horizon should be equal as stated in equation (1n). Moreover, the constraint (1o) presents the DOD calculation.

2.2. LP Model Based on BD Approach

To accelerate the optimization solution procedure, the proposed original optimization model is decomposed by means of BD approach. Accordingly, the sizing problem is split into a tractable master problem and sub-problems based on the illustrated flowchart in Fig. 3. The master problem deals with the DBESS investment planning problem and the sub-problem executes the robust optimal operation of distribution networks based on the results of the master problem. Here, it is considered that all buses of the system is capable of installing batteries.

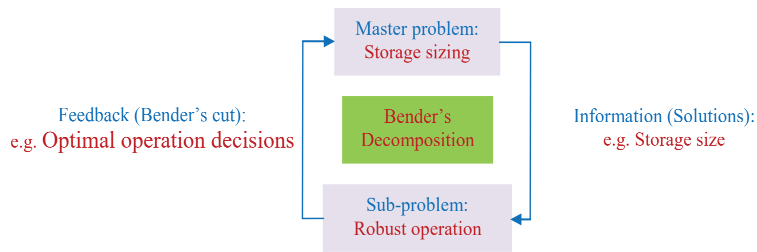

Fig. 3 Applying BD approach for the robust optimal sizing of the DBESSs

The BD is a commonly used optimization technique. J. F. Benders initially introduced the BD algorithm for solving large-scale MILP problems [30]. The basic idea is to separate integer variables and real variables or relax the tough constraints in the optimization model and treat larger optimization problems via decomposition in order to accelerate the calculation process. The BD algorithm has been successfully used in different ways to take the advantage of underlying problem structures for various optimization problems, such as network design, optimal transportation problem, plant location and stochastic optimization. In applying the BD algorithm, the original problem will be decomposed into a master problem and several sub-problems based on the LP duality theory. The sub-problems are the LP problems. The process of solving the master problem begins with only a few or no constraints. The sub-problems are used to determine if optimal solutions can be obtained under the remaining constraints based on this solution to the master problem. If feasible, we will get an upper bound solution of the original problem, while forming a new objective function (feasibility cut) for the next calculation of the master problem. If infeasible, a corresponding constraint (infeasibility cut), which is most unsatisfied, will be introduced to the master problem. Then, a lower bound solution of the original problem is obtained by re-solving the master problem with more constraints. The final solution based on the BD algorithm may require iterations between the master problem and the sub-problems. When the upper bound and the lower bound are sufficiently close, the optimal solution of the original problem is achieved [30].

While the original problem (1) is NLP, applying BD approach for this case may result in large duality gaps and it needs to use complementarity (equilibrium) constraints in the problem [22], accordingly, solving the proposed problem is hard. In the following subsections, an LP model is developed to guarantee obtaining the global optimal solution.

Master Problem: The DBESS planning is modeled in the master part as (2) to determine the sizing of DBESS (ω).

$$J_p = \min_{\omega} \; z_{lower} \tag{2a}$$

S.to:

$$z_{lower} \geq \sum_{b \in \varphi_b} c_b^s.\omega_b \tag{2b}$$

$$0 \leq \omega_b \leq \omega_{\max} \qquad \forall b \tag{2c}$$

$$z_{lower} \geq \sum_{b \in \varphi_b} c_b^s.\omega_b + J_{sub}^{(m)}(\lambda_{sub}^{(m)}, \mu_{sub}^{(m)}) \qquad \forall m = 1,2,...,n_f \tag{2d}$$

$$J_{sub}^{(r)}(\lambda_{sub}^{(r)}, \mu_{sub}^{(r)}) \leq 0 \qquad \forall r = 1,2,...,n_i \tag{2e}$$

The objective function of the master problem has been expressed in (2a) that is equal to the total investment cost of DBESSs in the smart distribution networks based on (2b). In other words, Equations (2a) and (2b) explain that the objective function, z_{lower}, is equal to $\sum_{b \in \varphi_b} c_b^s.\omega_b$, because, $a = b$ can be expressed as $a \geq b$ in the optimization problem with *min* term. Also, (2c) presents the size range of the DBESSs in the network. It is noted that (2b) and (2c) are called the "*initial master problem*". In the next step, the feasibility cut of (2d) is added to the initial master problem if the primal sub-problem or dual sub-problem is feasible [30], otherwise, the infeasibility cut of (2e) is fed to the initial master problem if the primal sub-problem is infeasible or the dual sub-problem is unbounded [30]. Accordingly, the output decision variable, ω, is calculated in the master problem and it is transmitted into the sub-problem as a constant parameter.

Sub-Problem: The objective function of the sub-problem is the sum of storage degradation cost, storage operational cost and storage revenue as mentioned in (1a) that should be minimized subject to (1b) to (1o) as constraints. This problem is NLP due to non-linear terms in (1d), (1e), storage degradation cost part of the objective function, and circular inequality constraints (1g) and (1h). Hence, it is expected that this problem obtain locally optimal solution due to non-convex formulation (1d) and (1e) at the high calculation time because the solver of NLP method is based on numerical analysis such as Newton Raphson [3, 31]. Therefore, in the next step, an equivalent linear model is developed as follows to obtain global optimal solation at the low calculation time:

– The linearized OPF model for the distribution networks is developed based on the first-order expansion of Taylor's series [3, 23]

– Circular inequality constraints are linearized based on a polygon approximation method [23, 32],

– The storage degradation cost part of the objective function is linearized based on the piecewise linearization method [26] according to Fig. 2.

Details of the above linearization processes have been explained in [3], [32] and [26], respectively. After applying these linearization techniques, the linear primal sub-problem can be written as follows:

$$J_{sub} = \min \overbrace{\sum_{t\in\varphi_t}\sum_{b\in\varphi_b} c_b^s.\omega_b.\gamma_{b,t}}^{Degradation\ cost\ of\ storage} + \overbrace{\sum_{t\in\varphi_t}\sum_{b\in\varphi_b} \lambda_t^{ch} P_{b,t}^{ch}}^{Operational\ cost\ of\ storage} - \overbrace{\sum_{t\in\varphi_t}\sum_{b\in\varphi_b} \lambda_t^{dis} P_{b,t}^{dis}}^{Revenue\ of\ storage} \tag{3a}$$

S.to:

$$PS_{b,t} - \sum_{j\in\varphi_b} A_{b,j} PL_{b,j,t} + \left(P_{b,t}^{dis} - P_{b,t}^{ch}\right) = PD_{b,t} - VRES_{b,t} : \lambda_{b,t}^{p} \quad \forall\, b, t \tag{3b}$$

$$QS_{b,t} - \sum_{j\in\varphi_b} A_{b,j} QL_{b,j,t} = QD_{b,t} : \lambda_{b,t}^{q} \quad \forall\, b, t \tag{3c}$$

$$PL_{b,j,t} = g_{b,j}\left(\sum_{l\in\varphi_l}\left(m_l - V^{\min}\right)\Delta V_{b,t,l} - V^{\min}\Delta V_{j,t,l}\right) - \left(V^{\min}\right)^2 b_{b,j}\left(\theta_{b,t} - \theta_{j,t}\right) : \lambda_{b,j,t}^{pl} \quad \forall b, j, t \tag{3d}$$

$$QL_{b,j,t} = -b_{b,j}\left(\sum_{l\in\varphi_l}\left(m_l - V^{\min}\right)\Delta V_{b,t,l} - V^{\min}\Delta V_{j,t,l}\right) - \left(V^{\min}\right)^2 g_{b,j}\left(\theta_{b,t} - \theta_{j,t}\right) : \lambda_{b,j,t}^{ql} \quad \forall b, j, t \tag{3e}$$

$$\theta_{b,t} = 0 : \lambda_t^{\theta} \quad \forall\, b = reference\,bus, t \tag{3f}$$

$$\cos\left(k\times\Delta\alpha\right)\times PL_{b,j,t} + \sin\left(k\times\Delta\alpha\right)\times QL_{b,j,t} \le SL_{b,j}^{\max} : \bar{\mu}_{b,j,t,k}^{sl} \quad \forall\, b, j, t, k \tag{3g}$$

$$\cos\left(k\times\Delta\alpha\right)\times PS_{b,t} + \sin\left(k\times\Delta\alpha\right)\times QS_{b,t} \le SS_b^{\max} : \bar{\mu}_{b,t,k}^{ss} \quad \forall\, b, j, t, k \tag{3h}$$

$$0 \le \Delta V_{b,t,l} \le \Delta V^{\max} : \bar{\mu}_{b,t,l}^{\Delta v} \quad \forall\, b, t, l \tag{3i}$$

$$E_{b,t} = E_{b,t-1} + \eta_{ch} P_{b,t}^{ch} - \frac{1}{\eta_{dis}} P_{b,t}^{dis} : \lambda_{b,t}^{e} \quad \forall\, b, t \tag{3j}$$

$$0 \le P_{b,t}^{ch} \le P_b^{ch-\max} : \bar{\mu}_{b,t}^{ch} \quad \forall\, b, t \tag{3k}$$

$$0 \le P_{b,t}^{ch} \le P_b^{dis-\max} : \bar{\mu}_{b,t}^{dis} \quad \forall\, b, t \tag{3l}$$

$$A_{\min}\omega_b \le E_{b,t} \le \omega_b : \underline{\mu}_{b,t}^{\omega}, \bar{\mu}_{b,t}^{\omega} \quad \forall\, b, t \tag{3m}$$

$$E_{b,0} = E_{b,T} : \lambda_b^{ec} \quad \forall\, b \tag{3n}$$

$$D_{b,t} = \left(1 - \frac{E_{b,t}}{\omega_b}\right) : \lambda_{b,t}^{dod} \quad \forall\, b,t \tag{3o}$$

$$\sum_{p \in P} X_{b,p} w_{b,t,p} = D_{b,t} : \lambda_{b,t}^{x} \quad \forall\, b,t \tag{3p}$$

$$\sum_{p \in P} Y_{b,p} w_{b,t,p} = \rho_{b,t} : \lambda_{b,t}^{y} \quad \forall\, b,t \tag{3q}$$

$$\sum_{p \in P} w_{b,t,p} = 1 : \lambda_{b,t}^{w} \quad \forall\, b,t \tag{3r}$$

$$\gamma_{b,t} \ge \rho_{b,t} - \rho_{b,t-1} : \underline{\mu}_{b,t}^{\gamma} \quad \forall\, b,t, \rho_{b,t-1} = 0\big|_{t=1} \tag{3s}$$

$$\gamma_{b,t} \ge 0 \quad \forall\, b,t \tag{3t}$$

The objective function of the sub-problem is the difference between the storage degradation and operation costs and revenue as (3a), wherein the term γ is the same as $\max\left(f\left(D_t\right) - f\left(D_{t-1}\right), 0\right)$ in (1a). Moreover, the equivalent linear forms of the constraints of (1d), (1e), (1g), and (1h) are as (3d), (3e), (3g), and (3h), respectively. Also, the storage degradation cost part of (1a) has been replaced (3a) with additional constrains of (3p) to (3t) wherein X_p and Y_p refer to the horizontal and vertical axis values of the points P_1 to P_6 in Fig. 2, and w is a binary variable to choose the right linear segment based on the piecewise linear approximation in Fig. 2. Also, The term ρ is the same as the $f(D)$. The other equations are similar to the linear constraints in (1). Noted that the λ and μ (in front of the constraints (3)) are dual variables of the constraints.

Note: Based on the reported results in [3, 23], the calculation error of the voltage and power using LP model with respect to the original NLP is about 0.5% and 2.5%, respectively. These error values are negligible for planning problems.

3. Robust Planning of DBESS

It is noted that the different parameters such load, vRES power, and charging/discharging energy price are uncertain. Hence, the stochastic, probabilistic and robust optimization techniques are needed to model these uncertain parameters. But, to achieve the sure solution, the stochastic and probabilistic models need high number of scenarios and knowledge about the probability distribution function of uncertain parameters [3, 22], hence, the computational burden of these models is greater than other optimization models. Therefore, the robust optimization is suitable due to low calculation time. The robust model obtains the optimal solution in the worst-case scenario which performs small feasibility space with respect to other scenarios of the stochastic model, thus, the situation of other scenarios can be satisfied with the results of the worst-case scenario. In addition, there are two main approaches for robust models: adaptive robust model [3, 22] and BURO [23]. The adaptive robust model needs to obtain the dual form of the primal formulation, where it finally obtains the bi-level model as a robust format of the original MILP problem [33]. But, the BURO to obtain robust model adds different linear constraints to the original LP or MILP models. Therefore, the BURO is a simple method and benefits from the low calculation time with respect to the other robust methods [23].

In this section, firstly, the general form of the robust optimization is presented and then the robust counterpart of the master and sub-problem is developed accordingly.

3.1. The BURO Model

The BURO considers the uncertainty level (σ) for all uncertain parameters. Thus, the true value of these parameters change between $(1 - \sigma)\times\left|\overline{P}\right|$ and $(1 + \sigma)\times\left|\overline{P}\right|$, where $\overline{P}$ is the forecasted value of the uncertain parameter [23]. Moreover, since the robust method is equal to the optimization of the worst-case scenario, and this scenario performs the small feasibility space with respect to the other scenarios, thus, the true value of the uncertain parameter is equal to its up-limit or down-limit due to the linear format of the proposed problem [23]. It should be noted that this condition depends on min/max term of an objective function, positive or negative coefficient of the uncertain parameter, the location of uncertain parameter in the objective function or constraint, left or right hand sides of the uncertain parameter location in the constraint. Consider the following MILP problem [23]:

$$\min_{x,y}/\max \quad c^T x + d^T y \tag{4a}$$

Subject to:

S.to:

$$Ex + Fy = e \tag{4b}$$

$$Ax + By \leq p \tag{4c}$$

$$\underline{x} \leq x \leq \overline{x} \tag{4d}$$

$$y \in \{0,1\} \tag{4e}$$

Where, the elements of matrixes A, B, p, i.e., $a_{i,m}$, $b_{i,n}$ and p_i, are considered as uncertain parameters, and these parameters are denoted as $\tilde{a}_{i,m}$, $\tilde{b}_{i,n}$ and $\tilde{p}_i$, respectively. Note that the indices of m, n and i are used for coefficients of the continuous (x) and binary (y) variables and uncertain parameter (p). Also, $a_{i,m}$, $b_{i,n}$ and p_i show the nominal or forecasted values of the uncertain parameters and the terms $\tilde{a}_{i,m}$, $\tilde{b}_{i,m}$ and $\tilde{p}_i$ are called "true" values of the uncertain parameters. It is noted that the true values of the uncertain parameters can be defined as follows in the proposed robust model [23]:

$$\left|\tilde{a}_{i,m} - a_{i,m}\right| \le \sigma\left|a_{i,m}\right|, \quad \left|\tilde{b}_{i,n} - b_{i,n}\right| \le \sigma\left|b_{i,n}\right|, \quad \left|\tilde{p}_i - p_i\right| \le \sigma\left|p_i\right| \tag{5}$$

where based on (5), the terms $\tilde{a}_{i,m}$, $\tilde{b}_{i,m}$ and $\tilde{p}_i$ are limited by upper and lower limits, and σ is the uncertainty level which is $\sigma > 0$. Finally, the solution (x, y) will be a robust solution if the following conditions are satisfied:

(i) The original problem, (4), has a feasible solution of (x, y),

(ii) For the $\tilde{a}_{i,m}$, $\tilde{b}_{i,m}$ and $\tilde{p}_i$ based on (5), the constraint (4c) with an error of at most $\delta \times \max[i, |p_i|]$ must be satisfied, where $\delta \ge 0$ is the feasibility tolerance and it allows a small amount of infeasibility in the uncertain inequality (4c) [23].

Therefore, the true value of different uncertain parameters are expressed as (6) to obtain the small feasibility space in the worst-case scenario based on the location and the coefficient sign, i.e., +1 or -1, of this parameter as well as min/max term of the objective function.

$$\tilde{a}_{i,m}x_m = a_{i,m}x_m + \sigma\left|a_{i,m}\right|\left|x_m\right|, \ \tilde{b}_{i,n}y_n = b_{i,n}y_n + \sigma\left|b_{i,n}\right|y_n, \ \tilde{p}_i = p_i - \sigma\left|p_i\right| \tag{6}$$

Then, the constraint (4c) for the true value of the uncertain parameter and the worst-case values of the uncertain parameters based on (6) is as follows:

$$\sum_{m \notin M1} a_{i,m}x_m + \sum_{m \in M1} \tilde{a}_{i,m}x_m + \sum_{n \notin K1} b_{i,n}y_n + \sum_{n \in K1} \tilde{b}_{i,n}y_n \le \tilde{p}_i + \delta.\max[i, |p_i|] \quad \forall i \tag{7}$$

Wherein, $M1$ and $K1$ are the set of indices of x and y, respectively, with uncertain coefficients in the i-th inequality constraint. Thus, (4c) for the worst-case values of the uncertain parameters can be written as follows:

$$\sum_{m\notin M1} a_{i,m}x_m + \sum_{m\in M1}\left(a_{i,m}x_m+\sigma\left|a_{i,m}\right|\left|x_m\right|\right)+\sum_{m\notin K1} b_{i,n}y_n+\sum_{m\in K1}\left(b_{i,n}y_n+\sigma\left|b_{i,n}\right|y_n\right) \le p_i-\sigma\left|p_i\right|+\delta.\max[i,\left|p_i\right|] \quad \forall i \tag{8}$$

Note that $|x_m|$ is defined by u_m as $-u_m \le x_m \le u_m$ to be added to (8). Finally, the BURO model for (4) with tuning parameters of σ and δ, RO(σ,δ), is as follows:

$$\min_{x,y}/\max \quad c^T x + d^T y \tag{9a}$$

S.to:

(4b) to (4e) (9b)

$$\sum_{m\notin M1} a_{i,m}x_m + \sum_{m\in M1}\left(a_{i,m}x_m+\sigma\left|a_{i,m}\right|u_m\right)+\sum_{m\notin K1} b_{i,n}y_n+\sum_{m\in K1}\left(b_{i,n}y_n+\sigma\left|b_{i,n}\right|y_n\right) \le p_i-\sigma\left|p_i\right|+\delta.\max[i,\left|p_i\right|] \quad \forall i \tag{9c}$$

$$-u_m \le x_m \le u_m \quad \forall m\in M1 \tag{9d}$$

3.2. The Proposed Robust Problem

In the proposed deterministic problem, (2) and (3), the charging and discharging price, λ^{ch} and λ^{dis}, active and reactive loads, *PD* and *QD*, and active power of vRES, are uncertain parameters. Accordingly, the proposed problem of (2) and (3) should be written as stochastic or robust models. Also, the model (2) includes only variable ω, as a "*here and now*" variable, that is independent of the uncertain parameters [34]. Consequently, the robust model is not implemented on the master problem (2). However, all the variables of the sub-problem (3) depend on the uncertain parameters that are called "*wait and see*" [34]. Therefore, the proposed robust model should be applied on the sub-problem. To this end, in the first step, the sub-problem should be converted into the standard form (4) to present the final robust model as follows:

$$J_{sub} = \min \; \overbrace{\sum_{t\in\varphi_t}\sum_{b\in\varphi_b} c_b^s.\omega_b.\gamma_{b,t}}^{Degradation\ \cos t\ of\ storage} + \overbrace{\beta_1}^{Operational\ \cos t\ of\ storage} - \overbrace{\beta_2}^{\mathrm{Re}venue\ of\ storage} \tag{10a}$$

S.to:

$$\sum_{t\in\varphi_t}\sum_{b\in\varphi_b} \lambda_t^{ch} P_{b,t}^{ch} \le \beta_1 : \mu^{\beta_1} \tag{10b}$$

$$\sum_{t\in\varphi_t}\sum_{b\in\varphi_b} \lambda_t^{dis} P_{b,t}^{dis} \le \beta_2 : \mu^{\beta_2} \tag{10c}$$

$$PS_{b,t} - \sum_{j\in\varphi_b} A_{b,j} PL_{b,j,t} + \left(P_{b,t}^{dis} - P_{b,t}^{ch}\right) \ge PD_{b,t} - VRES_{b,t} : \mu_{b,t}^{p} \quad \forall\, b, t \tag{10d}$$

$$QS_{b,t} - \sum_{j\in\varphi_b} A_{b,j} QL_{b,j,t} \geq QD_{b,t} : \mu_{b,t}^{q} \quad \forall\, b, t \tag{10e}$$

Eq. (3d) to Eq. (3t) (10f)

Where, equations (10a), (10b) and (10c) are equivalent to the objective function in (3a), because, β_1 and β_2 are equal to the left side of (10b) and (10c), respectively, while the J_{sub} is minimized. Moreover, (10d) and (10e) are in the form of $a \geq b$ that is equivalent to $a = b$ due to minimization of the objective function. Finally, the robust problem model is based on section 3.1 or RO(σ,δ) is as follows:

$$J_{sub} = \min \overbrace{\sum_{t\in\varphi_t}\sum_{b\in\varphi_b} c_b^{s}.\omega_b.\gamma_{b,t}}^{Degradation\ \cos t\ of\ storage} + \overset{Operational\ \cos t\ of\ storage}{\beta_1} - \overset{\mathrm{Re}venue\ of\ storage}{\beta_2} \tag{11a}$$

S.to:

$$\sum_{t\in\varphi_t} \lambda_t^{ch} \left(\sum_{b\in\varphi_b} P_{b,t}^{ch} \right) + \sigma \sum_{t\in\varphi_t} \lambda_t^{ch} u_t \leq \beta_1 : \mu^{r_{ch}} \tag{11b}$$

$$\sum_{t\in\varphi_t} \lambda_t^{dis} \left(\sum_{b\in\varphi_b} P_{b,t}^{dis} \right) + \sigma \sum_{t\in\varphi_t} \lambda_t^{dis} v_t \leq \beta_2 : \mu^{r_{dis}} \tag{11c}$$

$$-\sum_{b\in\varphi_b} P_{b,t}^{ch} \leq u_t \leq \sum_{b\in\varphi_b} P_{b,t}^{ch} : \underline{\mu}_t^{u}, \overline{\mu}_t^{u} \qquad \forall t \tag{11d}$$

$$-\sum_{b\in\varphi_b} P_{b,t}^{dis} \leq v_t \leq \sum_{b\in\varphi_b} P_{b,t}^{dis} : \underline{\mu}_t^{v}, \overline{\mu}_t^{v} \qquad \forall t \tag{11e}$$

$$PS_{b,t} - \sum_{j\in\varphi_b} A_{b,j} PL_{b,j,t} + \left(P_{b,t}^{dis} - P_{b,t}^{ch} \right) \geq \\ PD_{b,t} - VRES_{b,t} + \sigma \left| PD_{b,t} - VRES_{b,t} \right| - \delta \max \left\{ t, \left| PD_{b,t} - VRES_{b,t} \right| \right\} : \mu_{b,t}^{r_p} \quad \forall\, b, t \tag{11f}$$

$$QS_{b,t} - \sum_{j\in\varphi_b} A_{b,j} QL_{b,j,t} \geq QD_{b,t} + \sigma \left| QD_{b,t} \right| - \delta \max \left\{ t, \left| QD_{b,t} \right| \right\} : \mu_{b,t}^{r_q} \quad \forall\, b, t \tag{11g}$$

Eq. (10b) to Eq. (10f) (11h)

The above problem is called primal sub-problem, SP1. It is noted that the feasible region of SP1 will be changed by changing the output variables of the master problem [34]. Nevertheless, the dual form of SP1, named SP2, has a feasible region which is not dependent on the output variables of the master problem [34]. Therefore, the dual sub-problem (SP2) can be formulated as follows:

$$
J_{sub} = \max_{\lambda,\mu} \left\{ \begin{array}{l} \displaystyle\sum_{b\in\varphi_b} \left(E_{b,0}\lambda_b^{ec} + \sum_{t\in\varphi_t} \left(\begin{array}{l} \left(PD_{b,t} - VRES_{b,t}\right)\mu_{b,t}^{p} + QD_{b,t}\mu_{b,t}^{q} + P_b^{ch-\max}\overline{\mu}_{b,t}^{ch} + \\ P_b^{dis-\max}\overline{\mu}_{b,t}^{dis} + \omega_b\overline{\mu}_{b,t}^{\omega} + A_{\min}\omega_b\underline{\mu}_{b,t}^{\omega} + \lambda_{b,t}^{dod} + \lambda_{b,t}^{w} + \\ \left(PD_{b,t} - VRES_{b,t} + \sigma\left|PD_{b,t} - VRES_{b,t}\right| - \delta\max\left\{t,\left|PD_{b,t} - VRES_{b,t}\right|\right\}\right)\mu_{b,t}^{r_p} + \\ \left(QD_{b,t} + \sigma\left|QD_{b,t}\right| - \delta\max\left\{t,\left|QD_{b,t}\right|\right\}\right)\mu_{b,t}^{r_q} \end{array} \right) \right) \\ \displaystyle + \sum_{b\in\varphi_b}\sum_{t\in\varphi_t}\left(\sum_{l\in\varphi_l}\Delta V^{\max}\overline{\mu}_{b,t,l}^{\Delta v} + \sum_{k\in\varphi_k}\left(SS_b^{\max}\overline{\mu}_{b,t,k}^{ss} + \sum_{j\in\varphi_b} SL_{b,j}^{\max}\overline{\mu}_{b,j,t,k}^{sl} \right) \right) \end{array} \right\} \tag{12a}
$$

S.to:

$$
-\mu^{\beta_1} - \mu^{r_{ch}} \le 1 \ : \beta_1 \tag{12b}
$$

$$
-\mu^{\beta_2} - \mu^{r_{dis}} \le -1 \ : \beta_2 \tag{12c}
$$

$$
\sigma\lambda_t^{ch}\mu^{r_{ch}} + \underline{\mu}_t^{u} + \overline{\mu}_t^{u} = 0 \ : u_t \quad \forall t \tag{12d}
$$

$$
\sigma\lambda_t^{dis}\mu^{r_{dis}} + \underline{\mu}_t^{v} + \overline{\mu}_t^{v} = 0 \ : v_t \quad \forall t \tag{12e}
$$

$$
\mu_{b,t}^{p} + \mu_{b,t}^{r_p} + \sum_{k\in\varphi_k}\cos\left(k\times\Delta\alpha\right)\overline{\mu}_{b,t,k}^{ss} = 0 \ : PS_{b,t} \quad \forall b,t \tag{12f}
$$

$$
\mu_{b,t}^{q} + \mu_{b,t}^{r_q} + \sum_{k\in\varphi_k}\sin\left(k\times\Delta\alpha\right)\overline{\mu}_{b,t,k}^{ss} = 0 : QS_{b,t} \quad \forall b,t \tag{12g}
$$

$$
\lambda_{b,j,t}^{pl} - \sum_{b\in\varphi_b} A_{b,j}\left(\mu_{b,t}^{p} + \mu_{b,t}^{r_p}\right) + \sum_{k\in\varphi_k}\cos\left(k\times\Delta\alpha\right)\overline{\mu}_{b,j,t,k}^{sl} = 0 : PL_{b,j,t} \quad \forall b,j,t \tag{12h}
$$

$$
\lambda_{b,j,t}^{ql} - \sum_{b\in\varphi_b} A_{b,j}\left(\mu_{b,t}^{q} + \mu_{b,t}^{r_q}\right) + \sum_{k\in\varphi_k}\sin\left(k\times\Delta\alpha\right)\overline{\mu}_{b,j,t,k}^{sl} = 0 : QL_{b,j,t} \quad \forall b,j,t \tag{12i}
$$

$$
\mu_{b,t}^{p} + \mu_{b,t}^{r_p} + \mu^{\beta_2}\lambda_t^{dis} + \mu^{r_{dis}}\lambda_t^{dis} + \underline{\mu}_t^{v} - \overline{\mu}_t^{v} + \frac{1}{\eta_{dis}}\lambda_{b,t}^{e} + \overline{\mu}_{b,t}^{dis} \le 0 : P_{b,t}^{dis} \quad \forall\, b,t \tag{12j}
$$

$$
-\left(\mu_{b,t}^{p} + \mu_{b,t}^{r_p}\right) + \mu^{\beta_2}\lambda_t^{ch} + \mu^{r_{dis}}\lambda_t^{ch} + \underline{\mu}_t^{u} - \overline{\mu}_t^{u} - \eta_{ch}\lambda_{b,t}^{e} + \overline{\mu}_{b,t}^{ch} \le 0 : P_{b,t}^{ch} \quad \forall\, b,t \tag{12k}
$$

$$
\lambda_{b,t}^{e} - \lambda_{b,t+1}^{e} + \underline{\mu}_{b,t}^{\omega} + \overline{\mu}_{b,t}^{\omega} + z_b\lambda_b^{ec} + \frac{1}{\omega_b}\lambda_{b,t}^{dod} \le 0 : E_{b,t} \quad \forall\, b,t \quad \& \quad z_b = 1 \quad \forall t = T \tag{12l}
$$

$$
\lambda_{b,t}^{dod} + \lambda_{b,t}^{x} \le 0 : D_{b,t} \quad \forall\, b,t \tag{12m}
$$

$$
\lambda_{b,t}^{w} - X_{b,p}\lambda_{b,t}^{x} - Y_{b,p}\lambda_{b,t}^{y} \le 0 : w_{b,t,p} \quad \forall\, b,t,p \tag{12n}
$$

$$
\lambda_{b,t}^{y} - \underline{\mu}_{b,t}^{\gamma} + (1-y).\underline{\mu}_{b,t+1}^{\gamma} \le 0 : \rho_{b,t} \quad \forall\, b,t,\ y = 1\big|_{t=T} \tag{12o}
$$

$$
\underline{\mu}_{b,t}^{\gamma} \le c_b^{s}.\omega_b : \gamma_{b,t} \quad \forall\, b,t \tag{12p}
$$

$$\left(V^{\min}\right)^2\left(b_{b,j}\left(\lambda^{pl}_{b,j,t}-\lambda^{pl}_{j,b,t}\right)+g_{b,j}\left(\lambda^{ql}_{b,j,t}-\lambda^{ql}_{j,b,t}\right)\right)+s_b\lambda^{\theta}_t=0:\theta_{b,t} \qquad \forall b,j,t \quad \& \quad s_b=1 \quad \forall b=refrence\ bus \tag{12q}$$

$$\bar{\mu}^{\Delta v}_{b,t,l}-g_{b,j}\left(\left(m_l-V^{\min}\right)\lambda^{pl}_{b,j,t}-V^{\min}\lambda^{pl}_{j,b,t}\right)+b_{b,j}\left(\left(m_l-V^{\min}\right)\lambda^{ql}_{b,j,t}-V^{\min}\lambda^{ql}_{j,b,t}\right)\le 0:\Delta V_{b,t,l} \qquad \forall b,j,t,l \tag{12r}$$

$$\lambda=free,\ \bar{\mu}\ge 0,\ \underline{\mu}\le 0 \tag{12s}$$

Eq. (12) is the dual form of LP model of primal sub-problem. J_{sub} is the objective function of the dual problem, and the constraints (12b) to (12r) represent the dual constraints of the variables in the primal sub-problem which is indicated in the same equation. Constraint (12s) presents the limit of the dual variables which is determined by the constraints of the original problem.

3.3. BD Algorithm

There are three possible outcomes of solving SP2 based on the dual problem theory as follows [30]:

(i) SP2 is infeasible, thus, the original problem (1) is either infeasible or has an unbounded objective function. In this condition the process should be stopped.

(ii) SP2 has a feasible solution and its objective function is bounded. For this case, the feasibility cut (13) should be generated and added to the master problem of the previous iteration.

$$\text{Feasibility cut:}\quad z_{lower}\ge\sum_{b\in\varphi_b}c^s_b.\omega_b+J^{(m)}_{sub}(\hat{\lambda}_{sub},\hat{\mu}_{sub}) \qquad \forall J^{(m)}_{sub}(\hat{\lambda}_{sub},\hat{\mu}_{sub})=Eq.(12a)\Big|_{\hat{\lambda}_{sub},\hat{\mu}_{sub}} \tag{13}$$

(iii) SP2 has a feasible solution but its objective function is unbounded. Accordingly, SP3, (14) should be solved firstly, and in the next step, the infeasibility cut (15) should be generated and added to the master problem.

$$\mathbf{SP3}:J_{sub}=Eq.(12a)\Big|_{\Omega} \qquad \forall\Omega\triangleq\left\{\lambda,\mu\Big|Eq.(12a)\ to\ Eq.(12q),\lambda=[-1,1],\bar{\mu}=[1,\infty),\underline{\mu}=(-\infty,-1]\right\} \tag{14}$$

$$\text{Infeasibility cut:}\quad J^{(r)}_{sub}(\hat{\lambda}_{sub},\hat{\mu}_{sub})\le 0 \qquad \forall J^{(r)}_{sub}(\hat{\lambda}_{sub},\hat{\mu}_{sub})=Eq.(14)\Big|_{\hat{\lambda}_{sub},\hat{\mu}_{sub}} \tag{15}$$

where $\hat{\lambda}$ and $\hat{\mu}$ are optimal values of λ and μ in SP2/SP3. Also, noted that the situation of the objective function as infeasible, bounded and unbounded can be obtained by the optimization software such as GAMS, optimization toolbox of MATLAB and etc. In other words, these software especially GAMS determine the problem situation based on the solutions in its solvers [35]. Moreover, in each BD iteration, the feasibility or infeasibility cuts based on bounded or unbounded situation of SP2 are added to the master problem as (2d) or (2e), while the cuts in the previous BD iteration are not removed [30].

It is noted that the convergence criteria for the BD algorithm is to satisfy $\left|z_{upper} - z_{lower}\right| \leq \varepsilon$, where ε is the BD's convergence tolerance, and z_{upper} is the value of the objective function mentioned in (16). Noted that, the second part of (16) refers to J_{sub} for SP2. Also, the value of z_{lower} is determined in the last iteration based on the results of solving optimization problem of (2). That is, the BD convergence check is obtained if SP2 is feasible. The flowchart of implementing BD for the proposed problem is shown in Fig. 4.

$$z_{upper} = \sum_{b \in \varphi_b} c_b^s . \hat{\omega}_b + J_{sub}(\hat{\lambda}_{sub}, \hat{\mu}_{sub}) \qquad \forall J_{sub}(\hat{\lambda}_{sub}, \hat{\mu}_{sub}) = Eq.(12a)\Big|_{\hat{\lambda}_{sub}, \hat{\mu}_{sub}} \tag{16}$$

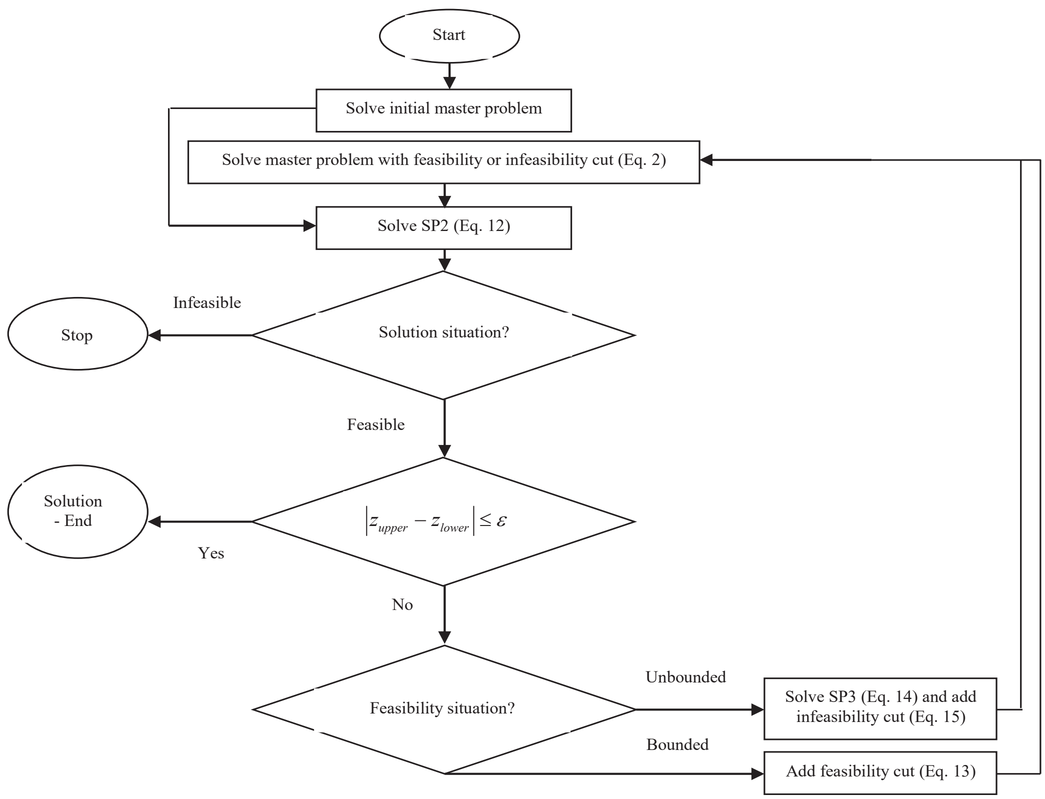

Fig. 4 BD algorithm to solve the proposed robust problem.

4. Numerical results and discussion

4.1. Data

The proposed storage planning framework is applied on the 19-bus MV CIGRE benchmark grid illustrated in Fig. 5 and its grid parameters such as bus incidence matrix, A, maximum loading of distribution line and station, SL^{max} and SS^{max}, and line conductance and susceptance, g and b, have been addressed in [21]. Also, some data is listed in Table II. Hourly load factor profiles of year 2016 [36] and charging/discharging prices of year 2017 [37] for

NordPool market in the zone Lithuania (LT) for one year are considered for this case study. Noted that the hourly active/reactive load is equal to multiplication of peak active/reactive load of house or bus and hourly load factor. In addition, this network includes high penetration rate of PV systems as vRES that are connected to each bus based on [12]. According to Table II, it is considered that the PV size can be changed between 10 to 20 kW in the different case studies, and also, the hourly power of each PV is equal to multiplication of PV size and hourly power percentage of PV that is addressed in [38]. Finally, it is noted that the proposed model does not require scenario samples. In other words, we need to forecast value of the uncertain parameter, and thus, the true value of the uncertain parameter in the worst-case scenario is obtained based on equation (7) and section 3.1.

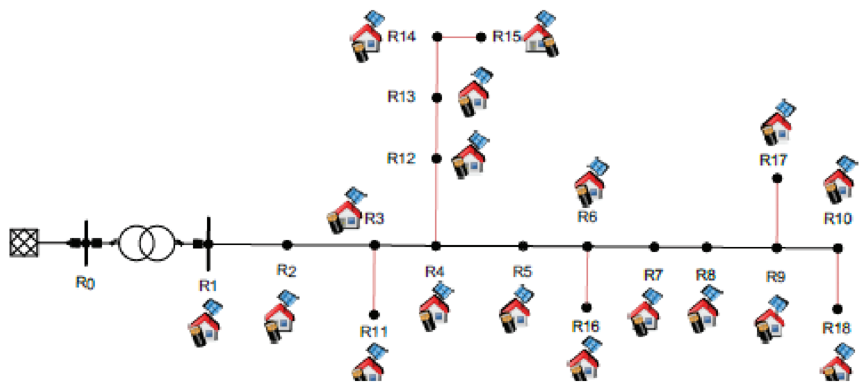

Fig. 5 19-bus MV CIGRE benchmark grid [21].

Table II: Problem data

No. of storage units	18
Maximum storage capacity or ω_{max} (kWh)	300
Storage roundtrip efficiency (charging and discharging)	0.88 [21]
Annual investment cost of storage (EUR/MWh/year)	5000 [21]
Charge and discharge rate (kW)	Maximum storage capacity [21]
A_{min} (%)	15%
Prediction horizon (hour)	8760
Year	1 year
Time step (hour)	1
Maximum power of PV (kW)	10 to 20
Power percentage profile of PV	Hourly pattern for one year based on [38]
Peak load of house (kW, kVAr)	(5, 1) [21]
Minimum and maximum voltage (per unit)	0.9 and 1.1 [21]
Base power (MVA)	0.5
Base voltage (kV)	0.4
X, Y	Based on Fig. 2 [26] for different points of *P*

4.2. Results

The proposed deterministic and robust models have been coded in GAMS 23.5.2 software and solved using the CPLEX solver in GAMS [35].

A. Convergence and Computation Time: In this section, the storage maximum capacity and PV capacity are considered 300 kWh and 20 kW, respectively. Moreover, the simulation of the proposed model is applied on one year with 8760 hours, and the objective function presents the annual profit of all storage systems. Also, number of linearization segments of the voltage magnitude term and circular constraints are equal to 5 and 30, respectively, in the LP model based on BD approach. Results of this section have been presented in Table III to compare different cases in NLP and LP based on the BD models, and Fig. 6 for investigating the BD convergence in the different robust models. Noted that Table III presents the capabilities of different solvers that are important factors in optimization problem. In other words, to obtain suitable solver to the proposed formulation, the convergence iteration, calculation time, objective function value and model status are checked for this problem. First and second factors refers to the calculation speed that should be high for a suitable solver, and other factors explain the situation of the optimal point that should be global optimal for the suitable solver. Moreover, this table can express the capability of the first contribution of this paper. As shown in Table III, the NLP solvers such as CONOPT, COUENNE, IPOPT, MINOS and SNOPT [35] have different results in convergence iteration, calculation time, objective function value and model status, while the total number of equations and variables is the same for all solvers. Also, the model status of NLP is locally optimal with the objective function value of 4102.562 EUR/year in the best condition that is occurred in IPOPT solver. But, the optimal situation with the lower value of the objective function (3331.220 EUR/year) has been obtained by LP model using BD approach, where the best solver for this case is CPLEX due to the low execution time with respect to the solvers of CBC and CONOPT [35]. Therefore, the LP model based on BD approach with the CPLEX solver is suitable and reliable for the proposed deterministic or robust problem model based on Table III.

Table III: Comparison of different solvers results for deterministic model

Model	Solver	Total number of equations	Total number of variables	Convergence iteration numbers	Calculation time (s)	Objective function (EUR/year)	Model status
NLP	CONOPT	5363547	3009801	390	461.437	5371.324	Locally optimal
	COUENNE	5363547	3009801	-	-	-	Infeasible
	IPOPT	5363547	3009801	54	517.845	4102.562	Locally optimal
	MINOS	5363547	3009801	412	2384.671	4864.483	Locally optimal
	SNOPT	5363547	3009801	-	-	-	Infeasible
LP based on BD	CPLEX	52*, 3006324**	20*, 7573638**	31	18.013	3331.220	Global optimal
	CBC	52*, 3006324**	20*, 7573638**	31	19.438	3331.220	Global optimal
	CONOPT	52*, 3006324**	20*, 7573638**	31	22.764	3331.220	Global optimal

* This number shows the number of the master problem's equations or variables (in the iteration that the problem is converged)

** This number shows the number of the sub-problem's equations (variables)

Fig. 6 shows the convergence progress of the proposed BD algorithm considering convergence tolerance, ε, equal to 0.5 $ for the different cases of the robust distributed storage planning problem. Based on this figure, the BD convergence iteration is 19, 31 and 36 for RO(σ,δ) = (0,0.02), (0.0) and (0.1,0), respectively. Note, RO(0,0.02), RO(0.0) and RO(0.1,0) express the impact of the feasibility tolerance (δ) in robust model, deterministic model, and impact of uncertainty level (σ) on the robust solution. Therefore, it can be said that RO(0,0.02) calculates the optimal solution with the lower number of iterations due to incresing feasibility space with respect to the feasibility space of the deterministic model. But, the feasibility space decreases in RO(0.1,0) with respect to the feasibility space of the deterministic model due to increased uncertainty level in comparison with the deterministic model. As a result, the number of iterations of the BD convergence is high in this robust model.

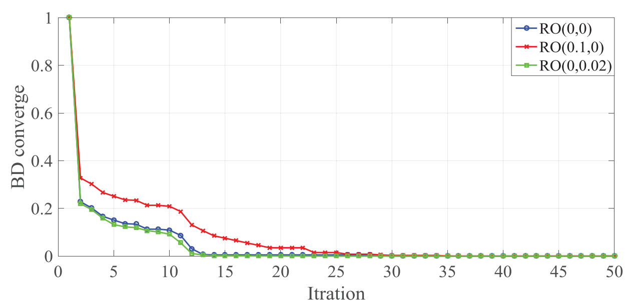

Fig. 6 BD convergence characteristic for different cases of the robust model

B. Uncertain Parameters: In this section, the values of the uncertain parameters in the different cases of the robust model are shown in Table IV. In the proposed robust model, the true value of uncertain parameter is obtained based on theory of section 3.1. Based on the Table IV, active and reactive loads as well as energy price (active power of PV) are decreased (increased) in the scenario with RO(0.1,0) with respect to the scenario of deterministic model, i.e., RO(0,0). Because, the uncertainty level (σ) has been increased in RO(0.1,0) in comparison with RO(0,0). Hence, it is expected that the value of profit, based on the sections 3.1 and 3.2, is reduced. It is noted that the proposed objective function, (1a), minimizes (maximizes) the total storage economic loss (profit), hence, it is expected that the profit will be high if discharging revenue of all storages is high and the total storage cost (charging, storage degradation and investment) is low. Discharging revenue of all storages will be increased if the active load and energy price increase and the active power of PV reduces. The reason is that the storage systems have stored the produced energy of their related PVs, thus the revenue is zero in this condition, nevertheless, in the case of supplying loads by the storage systems in the discharging mode, and then the revenue is not zero for such condition. In other words, the DBESSs generally charged by local PVs due to distribution operation limits, i.e. equations (1g) to (1i). Because, in the local energy (power) control method, the voltage deviation and overloading of distribution lines and main station are low [22-23]. Therefore, the storage system is charged by PVs when prices are low (high PV), and it will be discharged into loads when prices are high (no PV). Thus, the charging cost of DBESSs increases with increasing the PV power, and discharging revenue of DBESSs increases with increasing the load power and energy price. Also, the profit is low in the worst case scenario of RO(0.1,0) if the load and energy price (PV power) are decreased (increased).

In addition, the active and reactive loads as well as energy price (active power generations of PVs) are increased (decreased) in the scenario with RO(0,0.02) with respect to the scenario of deterministic model, RO(0,0), since, the feasibility tolerance (δ) is increased in RO(0,0.02) with respect to RO(0,0). It is noted that increasing δ will expand the feasibility region of the proposed problem, thus, it is expected that the profit will be improved, i.e., it is increased with respect to RO(0,0). Consequently, increasing δ will increase (reduces) the load and energy price (PV power).

Table IV: The value of uncertain parameters in different robust models for one year with PV capacity of 10 kW

Parameter	RO(0,0)	RO(0,0.02)	RO(0.1,0)
Total active load of network (pu)	5.584	5.695	5.025
Total reactive load of network (pu)	1.117	1.139	1.005
Total average active power of PVs (pu)	4.415	4.327	4.857
Total energy price (EUR/MWh)	446510.88	455441.098	401859.792

C. Sizing and Placement based on Distributed Strategy: In the distributed strategy, it is considered that the batteries can be installed in different buses of the system. Fig. 7 shows the total size of all distributed storage systems in the network based on the size of each PV and the maximum storage capacity (MSC) for different cases of the robust model. In the case of RO(0,0) without considering the storage degradation as seen in Fig. 7(a), the total size of all distributed storage systems is constant if PV size is changed from 0 to 12 kW. However, this value will be reduced for the PV size above 12 kW in the part with "*Profit of Storage* > 0" because the system operation limits, i.e., (1g) to (1i), constrain the increment of the size of some distributed storage systems in these conditions based on Fig 7(b). In Fig. 7(b), four cases have been implemented where case I refers to the proposed problem with network constraints, and cases II to IV express the proposed problem without voltage limit, the proposed problem without line flow limit, and the proposed problem without voltage and line flow limits, respectively. It is noted that in this test system, based on the real data for electricity prices taken from [37], the prices are high even if the PV production is high. Also, it is noted that here it is assumed that the owners of the battery and the PV are not the same. Accordingly, if a distributed locational marginal pricing is used in the grid, i.e., taking the nodal prices directly from the duals of the load balances in the model, we will get different conclusions, since the price of power would be low when the PV production is high. As seen in Fig. 7 (b), if the system operation limits such as voltage, line flow and station power limits are ignored from the proposed problem, then, the total size of all distributed storage systems would be equal to 18×MSC, where 18 is the number of storage locations. Therefore, it can be said that the system operation limits are important in specifying the total size of all distributed storage systems. Moreover, it is noted that the charging cost will increase if the local PV size is increased, because, in the case of increasing the capacity of PVs, the PV power will be more than the load, and the local power control can provide a suitable voltage profile and will reduce the power flowing of distribution lines and the main station [31]-[32]. Hence, the excess energy of the PVs will be stored in the storage systems, thus, the charging cost of the storage systems based on Eq. (1a) will be increased. Also, during the discharging mode, the revenue of the storage systems will be reduced in this condition, because, the more portion of the supplied energy to loads is generated by PVs. Therefore, it is possible to have negative profit for the storage systems. Accordingly, the larger sizes of the total distributed storage systems would not be suitable in the larger sizes of PVs. This statement has been shown in Fig. 7(a) in the part with "*Profit of Storage* < 0". Thus, based on these statements, it can be said that:

– If the PV size is more than the load demand, thus in this condition, the extra PVs work as a reserve and it is not required to install any storage in the system. Accordingly, by increasing the PV size, the storage capacity will be decreased.

– If the PV size is less than load demand, then there are two main states:

  i. *Availability of enough power flow capacity of feeders*: in this state, by increasing the PV capacity, the required storage will be constant or increased depending on the investment costs.

  ii. *Limited power flow capacity of feeder*: in this case, by increasing the PV capacity, while the feeders are congested, then the availability of the storage is not beneficial. Accordingly, by increasing the PV size, the storage capacity will be decreased.

In addition, the total size of all distributed storage systems is increased if the MSC increases based on Fig. 7(a). Finally, it is noted that the PV size (PVmax) will be increased if the MSC increases as shown in the section of "*Profit* = 0" in Fig. 7(a). Because, the profit of the right side of this curve is negative, thus, it can be inferred that in the curve with "*Profit* = 0", the PV size is the maximum for different values of MSC.

Fig. 7(c) shows the total size of all distributed storage systems in the network versus PV size for different cases of the robust model. Based on this figure, the storage size of the cases RO(0,0) with/without considering the storage degradation is the same. Nonetheless, the storage size will be increased (reduced) if δ (σ) increased. Also, the maximum PV size is high and low in the cases of RO(0,0.02) and RO(0.1,0), respectively. In other words, according to Fig. 7(b), the profit of the storage is non-positive (≤ 0) if the PVmax is more than 22, 20, 23 and 19 kW for the cases RO(0,0) without storage degradation, RO(0,0), RO(0,0.02), and RO(0.1,0), respectively.

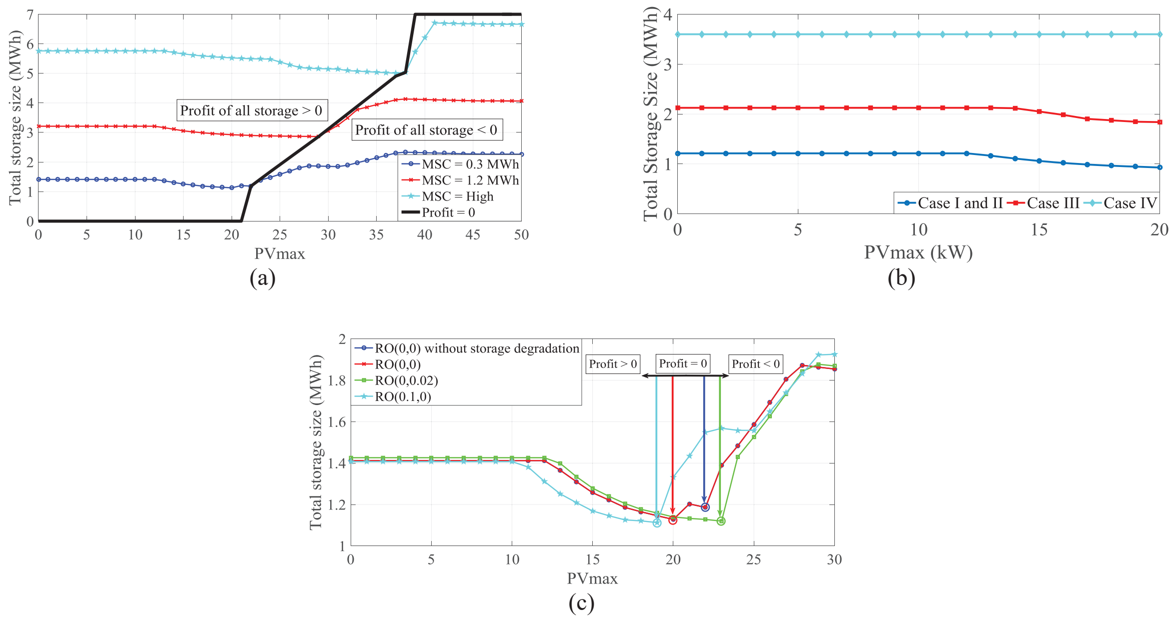

Fig. 7 Total size of all distributed storage systems in the network versus PV sizes, (a) RO(0,0) without storage degradation, (b) RO(0,0) without storage degradation while considering different cases for system operation limits MSC = 0.2 MWh (c) robust models

In Table V, the annual investment and charging as well as the degradation costs, annual discharging revenue and annual profit of all distributed storage systems are depicted for different robust models. Based on this table, the annual investment cost of the storage will be increased in the case of higher maximum capacities. But, the annual investment cost and storage size are reduced by increasing the PV size or PV penetration rate in different robust models. Because based on Fig. 7(a), the total size of all DBESSs is increased for the higher maximum storage capacities and it would be decreased by increasing the size of PV. In addition, increasing PV penetration rate and MSC in the different robust models cause that the annual charging cost and discharge revenue of the all distributed storage systems increase based on Table V.

Indeed, the charging power of storage systems is increased if the PV penetration rate is increased to satisfy the constraints Eq. (1g) to Eq. (1i), and the discharging power of storage systems is increased to minimize the objective function Eq. (1a) and to satisfy the constraints Eq. (1g) to Eq. (1i). Moreover, the degradation cost of all storage systems is reduced (increased) if PVmax (MSC) increases.

Table V: Comparison of economic results for the distributed storages

Model	RO(0,0) without storage degradation				RO(0,0)			
MSC (MWh)	0.15		0.30		0.15		0.30	
PVmax (kW)	10	20	10	20	10	20	10	20
Investment cost (EUR/year)	5562	4138	7062	5638	5562	4138	7062	5638
Charging cost (EUR/year)	12298	20264	15414	23380	12298	20264	15414	23380
Degradation cost (EUR/year)	-	-	-	-	8	7.2	10.5	10.1
Discharging revenue (EUR/year)	26487	25138	33714	32365	26478	25128	33702	32351
Profit (EUR/year)	8627	736	11238	3347	8610	719	11216	3323
Model	RO(0,0.02)				RO(0.1,0)			
MSC (MWh)	0.15		0.30		0.15		0.30	
PVmax (kW)	10	20	10	20	10	17	10	19
Investment cost (EUR/year)	5674	4202	7125	5702	5243	4128	7232	6145
Charging cost (EUR/year)	12145	19795	15231	22973	12429	16498	16241	23715
Degradation cost (EUR/year)	8	7.2	10.5	10.1	8.2	7.35	10.65	10.26
Discharging revenue (EUR/year)	26873	25469	34233	32840	24451	21771	30966	30224
Profit (EUR/year)	9046	1465	11867	4155	6771	1138	7432	352

In comparison between cases RO(0,0) without and with storage degradation, the investment and charging cost of the storage systems is the same based on Table V, and the discharging revenue is reduced in RO(0,0) with respect to the RO(0,0) without storage degradation. Because, the discharging mode or contribution of the storage system will be reduced in RO(0,0) with respect to the RO(0,0) without storage degradation due to the second part of Eq. (1a). Hence, the discharging power, P^{dis}, and discharging revenue only change in RO(0,0) in comparison with RO(0,0) without storage degradation. Also, there is a degradation cost in RO(0,0), therefore, the storage systems profit in RO(0,0) is less than RO(0,0) without storage degradation. Moreover, the charging cost of the storage systems reduces/increases in RO(0,0.02)/RO(0.1,0), and the investment cost and discharging revenue of storage systems reduces/increases in RO(0.1,0)/RO(0,0.02). For the reason that the load and energy price/PV power increases with increasing δ/σ and reduces with increasing σ/δ based on Table IV. Therefore, charging cost/discharging revenue and investment cost are increased with increasing σ/δ. Also, the degradation cost is almost the same in cases RO(0,0), RO(0,0.02) and RO(0.1,0).

D. Sizing and Placement Based on Centralized Strategy: In this strategy, it is considered that one battery can be installed in the optimal location of the system. Hence, Eq. (2c) rewritten as $0 \le \omega_b \le \omega_{\max} xs_b$, where *xs* is a binary variable for the storage installation. Thus, the storage installed if *xs* = 1, otherwise, it is not installed. Moreover, the constraint of $\sum_b xs_b = 1$ should be added to the master problem, Eq. (2), for the centralized strategy. Therefore, the output variables of the master problem are *xs* and ω. Based on this strategy, the results of the centralized storage systems planning have been expressed in Table VI and Fig. 8. In Table VI, the optimal location of storage system is bus 1 for different cases of the robust model for the smaller sizes of the PVs, but, the location of the storage will be changed to bus 4 in the larger sizes of the PVs for different cases of the robust models. According to the try-and-error approach (similar to the analysis in Fig. 7(c) for the distributed strategy), the maximum PV sizes in the centralized strategy are determined to be 18.3, 18.2, 18.8 and 16 kW for cases of RO(0,0) without storage degradation, RO(0,0), RO(0,0.02) and RO(0.1,0), respectively. Based on these assumptions, as results of Table VI show, in the case of PVmax = 10 kW, the investment and charging costs of the storage systems are the same for the cases of RO(0,0) without storage degradation and RO(0,0), while the discharging revenue has been reduced in RO(0,0) with respect to the RO(0,0) without storage degradation. Also, there is a degradation cost in RO(0,0), therefore, the storage systems profit in RO(0,0) is less than RO(0,0) without the storage degradation. Moreover, the charging cost of the storage systems has been reduced/increased in RO(0,0.02)/RO(0.1,0), and the investment cost and discharging revenue of the storage systems have been reduced/increased in RO(0.1,0)/RO(0,0.02), respectively. Also, the degradation cost is almost the same in cases RO(0,0), RO(0,0.02) and RO(0.1,0). Consequently, as results of Table VI show the profit of the storage is based on different costs and revenues.

Table VI: Comparison of economic results for the centralized storages

Model	RO(0,0) without storage degradation		RO(0,0)		RO(0,0.02)		RO(0.1,0)	
MSC (MWh)	Inf		Inf		Inf		Inf	
PVmax (kW)	10	18.3*	10	18.2*	10	18.8*	10	16*
Optimal location (bus)	1	4	1	4	1	4	1	4
Optimal storage capacity (MWh)	3.262	0.543	3.262	0.545	3.275	0.546	3.250	0.532
Investment cost (EUR/year)	16311	2717	16311	2727	16516	2731	16250	2659
Charging cost (EUR/year)	37587	13900	37587	13668	38249	14326	34223	11733
Degradation cost (EUR/year)	-	-	22.26	24.67	22.2	24.75	22.6	24.47
Discharging revenue (EUR/year)	77447	16658	77440	16586	78842	17109	70383	13432
Profit (EUR/year)	23550	41	23523	168	23995	28	19907	15

* the maximum value of PVmax in different cases of the robust model

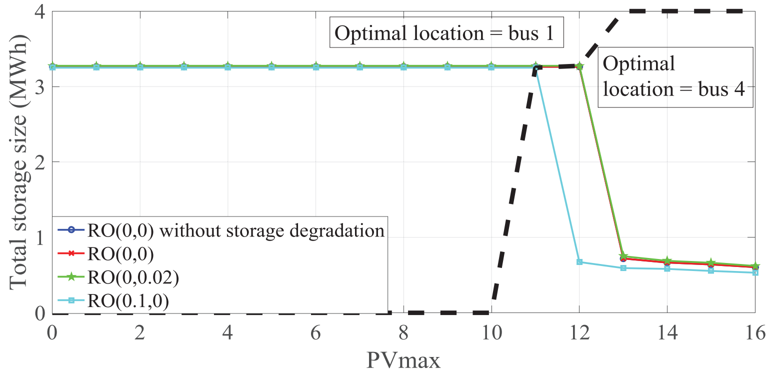

Fig. 8 Size of centralized storage system based on PV size for different robust models

Fig. 8 shows the storage system size versus the PV size for the case that the optimal location of the storage system is bus 1 for the PV size between 0-12 kW at cases RO(0,0) without the storage degradation, RO(0,0) and RO(0,0.02), and it is bus 1 for the PV size between 0-11 kW at RO(0.1,0). Also, the storage size is constant for the PV size between 0-12 kW and 0-11 kW at cases RO(0,0) without the storage degradation, RO(0,0) and RO(0,0.02), and RO(0.1,0), respectively. In the Fig. 8, the graph has been split into two regions by a dotted line. Indeed, the left side and right side of the dotted line refer to the regions that the optimal location of the storage is bus 1 and bus 4, respectively. Also, it is observed in the figure that the storage sizes are reduced if the PV size goes above 12 or 11 kW for cases RO(0,0) without the storage degradation, RO(0,0) and RO(0,0.02), and RO(0.1, 0), respectively.

E. Investigating Network Indexes and Flexibility: For this purpose, at first, the main assumptions for this study are: maximum size of the storages is 150 kWh for two days (48 hours), the maximum power of PVs is 10 kW, and the load percentage, energy price and PV power percentage are based on the data of 30 Sept. and 1 Oct. 2017 in [36]-[38]. Also, it is assumed that the objective function of (3a) has been changed to the minimization of the voltage deviation using $\sum_{b\in\varphi_b}\sum_{t=1}^{48}\left(V_{b,t}-V_{ref}\right)^2$ to investigate the effects of charging/discharging profile of storages on the network indexes. Considering this objective function will affect the storage profile in a way to improve network indexes and enhance PV penetration conditions. Based on the above assumptions, the simulations have been executed and the results have been illustrated in Fig. 9. In this study, four cases are considered: network without PV and storage, network with PV and without storage, and network with PV and storage for RO(0,0), RO(0.1,0) and RO(0,0.02). As shown in Fig. 9(a), the PVs inject their generations in the periods of 10:00–17:00 of 30 Sept. and 9:00–16:00 of 1

Oct. This fact results in the higher network active power loss and increased voltage profile in these periods in case of network without the storage system with respect to the case we have only network as shown by Figs. 9(b) and (c). However, adding storage in cases RO(0,0), RO(0.1,0) and RO(0,0.02), has improved the profiles of the voltage and active power loss and station power as shown in Fig. 9. For the reason that, in the low load conditions, the PVs have charged the storage system in the cases RO(0,0), RO(0.1,0) and RO(0,0.02), and the storages injects back the stored energy to the network in peak load times as shown in Fig. 9 (d). Indeed, as Fig. 9(d) shows the storage systems are charged in period of 10:00 to 17:00 of 30 Sept. and 9:00 to 16:00 of 1 Oct. by PVs based on Fig. 9(a). Also, the storage systems inject the energy back to the network in periods of 18:00 of 30 September to 8:00 of 1 October and 17:00 to 24:00 of 1 October. Accordingly, the load profile is flat, where this statement shows the high flexibility in cases RO(0,0), RO(0.1,0) and RO(0,0.02). Besides, the storage has been operated in a way that the active power of the station, active power loss and voltage in cases RO(0,0.02) and RO(0.1,0) have been increased with respect to RO(0,0) for some hours, and decreased in some other hours as shown by Fig. 9(a)-(c). This is because of the existing uncertain parameters in different robust models. Likewise, the daily pattern of the stored energy in all storage systems is almost the same for cases RO(0,0) and RO(0,0.02), but it is increased/decreased at periods 1:00-35:00/36:00-48:00 in RO(0.1,0) with respect to the cases of RO(0,0) and RO(0,0.02).

The comparison results of both centralized and distributed strategies of placing storage systems in the network have been addressed in Table VII. As table VII shows, in the case of unlimited capacity assumption for the storage systems for both strategies, the maximum size of PV is 18 and 38 kW (according to the try-and-error approach), and the total storage size (obtained by the optimization) is 0.583 and 5.033 MWh for the centralized and distributed storage systems, respectively. Therefore, it is said that the distributed strategy causes that the proposed distribution network supports the high PV size; hence, it needs a high size for total DBESSs. But, the centralized strategy which considers one ESS in the distribution network cannot obtain high capacity for ESS due to the system operation limits, (1g)-(1i). Thus, this strategy achieves low penetration rate of PVs with respect to the distributed strategy. In addition, the results confirm the superiority of the distributed strategy for placing storage systems in terms of the voltage deviation and energy loss with respect to the centralized storage planning that is proposed in [4-8]. In other words, the minimum voltage deviation, i.e. $\sum_{b\in\varphi_b}\sum_{t=1}^{48}\left(V_{b,t}-V_{ref}\right)^2$, is equal to 0.1011 pu in the distributed storage planning, but, it is equal to 0.2231 pu for the centralized storage planning. Also, the annual energy loss of the proposed distribution network is 2647.5 and 3476.3 kWh based on the centralized and distributed strategies, respectively. Therefore, the minimum voltage deviation and annual energy loss in the distributed method is less than the centralized storage planning about 54.7% and 23.8%, respectively due to the high size of PV and storage in the distributed method in comparison with the centralized method.

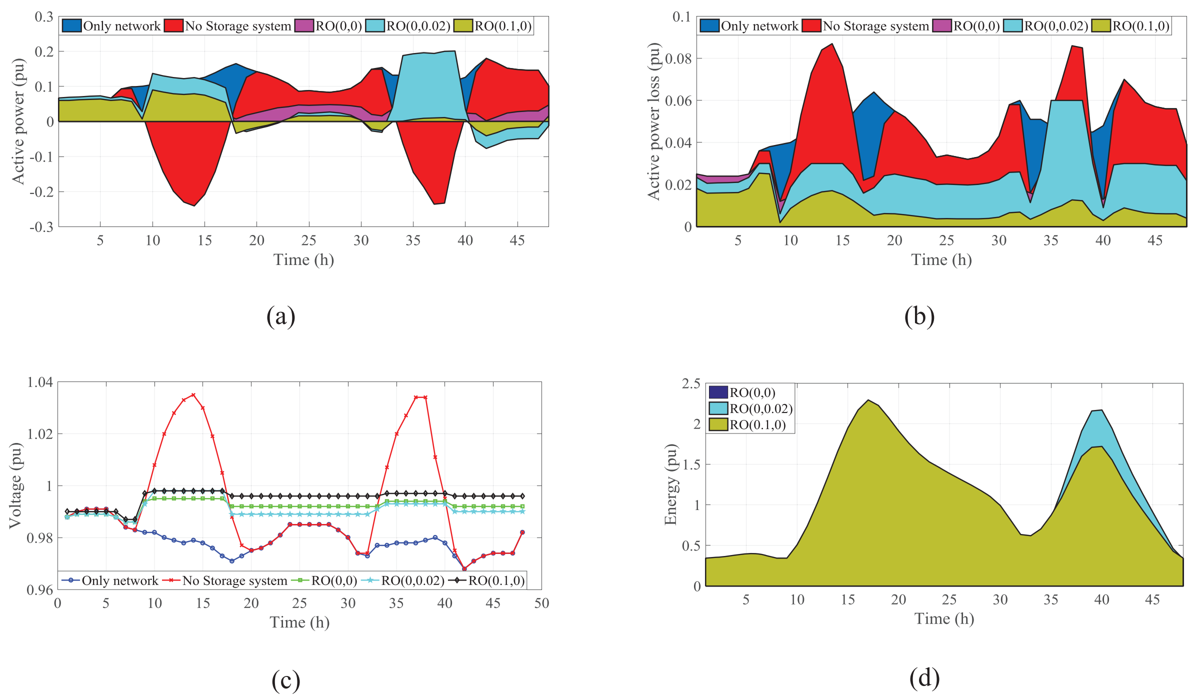

Fig. 9 Effects of storages on the network indexes: (a) daily pattern of active power of station bus, (b) daily pattern of network active power loss, (c) daily pattern of mean voltage of network buses, (d) daily pattern of the stored energy in all storage systems.

Table VII: Comparison of centralized and distributed storage planning strategies

Case	Centralized storage planning	Distributed storage planning
Maximum storage capacity (kWh)	Inf.	Inf .
Maximum size of PV (kW)	18	38
Total storage size (MWh)	0.583	5.033
Minimum voltage deviation, i.e., $\sum_{b\in\varphi_b}\sum_{t=1}^{48}\left(V_{b,t}-V_{ref}\right)^2$, (pu)	0.2231	0.1011
Annual energy loss (kWh)	3476.3	2647.5

5. Conclusions

This paper presents a robust planning method for DBESSs from the viewpoint of DSO to increase the network flexibility. Accordingly, based on the proposed deterministic robust model, the difference between the DBESS investment, degradation and operation (charging) costs and revenue of DBESS for selling its discharged power is minimized as the objective function. Also, this problem is subjected to the AC power flow equations, limits of network indexes, vRES and DBESSs constraints. The original problem is in the form of NLP, accordingly, the equivalent LP model based on the BD approach has been proposed using the first-order expansion of Taylor's series for linearization of power flow equations and the polygon for linearization of circular inequality. Results imply that the LP model based on the BD approach can obtain optimal solution with an acceptable calculation speed. In addition, to deal with the uncertainties (including active and reactive load, energy or charging/discharging price and output power of RESs), a BURO model has been developed. Storage system size is high/low in low/high value of PV size. Considering the theoretical properties of the proposed model and the results of the case studies carried out, the conclusions below are as follows:

– The obtained results underscore the importance of considering distributed strategy for placing storages in the distribution networks. Therefore, one should be aware that a system with enough installed storage capacity to cover power mismatches in the case of uncertain renewable energy sources, may not be able to utilize the available storage capacity in real time-operation due to congestions in the network.

– The obtained results illustrate that sizing and sitting of DBSSs highly depend on the adjusting parameters of the uncertainty in the robust models. That is, by increasing the uncertainty level and/or decreasing the feasibility tolerance of the robust optimization problem, the storage capacity is reduced.

– Simulation results imply that different electricity pricing mechanisms can affect the battery sizing for different levels of PV penetrations in the system.

– The results pinpoint the necessity of an accurate AC power flow method for an economically efficient system operation, mainly due to considering the system operation limit such as voltage, line flow and station power limits.

– Moreover, the DBESSs can improve the network and flexibility indices such as voltage, power loss and network power profiles, with respect to the centralized storage system. Noted that, this strategy could also be a suitable scheme to utilize the possible benefits of the mobile storages of electric vehicles (EVs) in parking lots which are located in different sites of the distribution networks.

A research work is underway to also include the storage planning problem in the smart distribution network in the presence of vRES and EVs. In this regard, it could also be studied whether battery storage configurations in accordance with demand response capability of prosumers are more preferable. Also, EVs parking lot can play storage role in distribution planning to improve the network flexibility and reduce the DBESS's cost. In addition, the proposed flexible storage planning can be implemented on real world data or real distribution network, in the event that the smart grid concept and technologies are provided to the distribution system. Also, the proposed method can obtain more benefits for the end user that is home customer in this paper. Because, each customer can install PV and ESS in its load point, hence, it supplies its load and it can obtain revenue by energy selling to the network in the market formwork. Therefore, to cope with this issue, we investigate the storage planning problem from the viewpoint of different customers in the future works based on the real data in Iran for distribution networks, energy price, and vRES.

Acknowledgments

Parts of the research leading to these results has received funding from the European Union under the Horizon2020 Framework Programme, grant agreement no. 731148 (INVADE H2020 project).

References

[1] Eurelectric, Flexibility and Aggregation Requirements for their interaction in the market, *Eurelectric*, 2014.

[2] S.Ø. Ottesen, P. Olivella-Rosell, P. Lloret, A. Hentunen, P. Crespo del Granado, S. Bjarghov, V. Lakshmanan, J. Aghaei, M. Korpås and H. Farahmand, "Simplified Battery operation and control algorithm," Deliverable D5.3, EU-INVADE, 2017.

[3] S. Pirouzi, J. Aghaei, V. Vahidinasab, T. Niknam, and A. Khodaei, "Robust linear architecture for active/reactive power scheduling of EV integrated smart distribution networks," *Electric Power System Research*, vol. 155, pp. 8-20, 2018.

[4] R. Hemmati, H.t Saboori, "Emergence of hybrid energy storage systems in renewable energy and transport applications – A review," *Renewable and Sustainable Energy Reviews*, vol. 65, pp. 11-23, 2016.

[5] F. Díaz-González, A. Sumper, O. Gomis-Bellmunt, R. Villafáfila-Robles, "A review of energy storage technologies for wind power applications," *Renewable and Sustainable Energy Reviews*, vol. 16, pp. 2154-2171, 2012.

[6] H. Zhao, Q. Wu, S. Hu, H. Xu, C.N. Rasmussen, "Review of energy storage system for wind power integration support," *Applied Energy*, vol. 137, pp. 545-553, 2015.

[7] M. Beaudin, H. Zareipour, A. Schellenberglabe, W. Rosehart, "Energy storage for mitigating the variability of renewable electricity sources: An updated review," Energy for Sustainable Development, vol. 14, pp. 302-314, 2010.

[8] D.O. Akinyele, R.K. Rayudu, "Review of energy storage technologies for sustainable power networks," Sustainable Energy Technologies and Assessments, vol. 8, pp. 74-91, 2014.

[9] J. Qiu, J. Zhao, H. Yang, D. Wang, Z.Y. Dong, "Planning of solar photovoltaics, battery energy storage system and gas micro turbine for coupled micro energy grids," *Applied Energy*, vol. 219, pp. 361-369, 2018.

[10] M.R. Jannesar, A. Sedighi, M. Savaghebi, J.M. Guerrero, "Optimal placement, sizing, and daily charge/discharge of battery energy storage in low voltage distribution network with high photovoltaic penetration," *Applied Energy*, vol. 226, pp. 957-966, 2018.

[11] J. Cervantes, F. Choobineh, "Optimal sizing of a nonutility-scale solar power system and its battery storage," *Applied Energy*, vol. 216, pp. 105-115, 2018.

[12] E. Grover-Silva, R. Girard, G. Kariniotakis, "Optimal sizing and placement of distribution grid connected battery systems through an SOCP optimal power flow algorithm," *Applied Energy*, vol. 219, pp. 385-393, 2018.

[13] M. Bucciarelli, S. Paoletti, A. Vicino, "Optimal sizing of energy storage systems under uncertain demand and generation," *Applied Energy*, vol. 225, pp. 611-621, 2018.

[14] R. Li, W. Wang and M. Xia, "Cooperative planning of active distribution system with renewable energy sources and energy storage systems," *IEEE Access*, vol. 6, pp. 5916-5926, 2018.

[15] Y. Xiang, W. Han, J. Zhang, J. Liu and Y. Liu, "Optimal sizing of energy storage system in active distribution networks using fourier–legendre series based state of energy function," *IEEE Transactions on Power Systems*, vol. 33, no. 2, pp. 2313-2315, March 2018.

[16] M. Nick, R. Cherkaoui and M. Paolone, “Optimal planning of distributed energy storage systems in active distribution networks embedding grid reconfiguration,” *IEEE Transactions on Power Systems*, vol. 33, no. 2, pp. 1577-1590, March 2018.

[17] M. Sedghi, A. Ahmadian and M. Aliakbar-Golkar, “Optimal storage planning in active distribution network considering uncertainty of wind power distributed generation,” *IEEE Transactions on Power Systems*, vol. 31, no. 1, pp. 304-316, Jan. 2016.

[18] Y. Zhang, S. Ren, Z.Y. Dong, Y. Xu, K. Meng, and Y. Zheng, “Optimal placement of battery energy storage in distribution networks considering conservation voltage reduction and stochastic load composition,” *IET Generation, Transmission & Distribution*, vol. 11, no. 15, pp. 3862-3870, 10 19 2017.

[19] A. Meechaka, A. Sangswang, K. Kirtikara, and D. Chenvidhya, “Optimal location and sizing for PV system and battery energy storage system using ABC algorithm considering voltage deviation and time of use rate,” *9th International Conference on Information Technology and Electrical Engineering (ICITEE)*, Phuket, pp. 1-6, 2017.

[20] E. Nasrolahpour, S.J. Kazempour, H. Zareipour, and W. D. Rosehart, “Strategic sizing of energy storage facilities in electricity markets,” *IEEE Transactions on Sustainable Energy*, vol. 7, no. 4, pp. 1462–1472, 2016.

[21] P. Fortenbacher, A. Ulbig, and G. Andersson, “Optimal Placement and Sizing of Distributed Battery Storage in Low Voltage Grids using Receding Horizon Control Strategies,” *IEEE Transactions on Power Systems*, vol. 33, no. 3, May 2017.

[22] S. Pirouzi, J. Aghaei, M.A. Latify, G.R. Yousefi, and G. Mokryani, “A robust optimization approach for active and reactive power management in smart distribution networks using electric vehicles,” *IEEE System Journal*, pp. 1-12, 2017.

[23] S. Pirouzi, J. Aghaei, T. Niknam, M. Shafie-khah, V. Vahidinasab, and J.P.S. Catalão, “Two alternative robust optimization models for flexible power management of electric vehicles in distribution networks,” *Energy*, vol. 141, pp. 635-652, 2017.

[24] J. Kim, Y. Choi, S. Ryu, and H. Kim, “Robust operation of energy storage system with uncertain load profiles,” *Energies*, vol. 10, pp. 1-15, 2017.

[25] R.A. Jabr, I. Džafić, and B.C. Pal, “Robust optimization of storage investment on transmission networks,” *IEEE Transactions on Power Systems*, vol. 30, no. 1, pp. 531-539, 2015.

[26] M.A. Ortega-Vazquez, “Optimal scheduling of electric vehicle charging and vehicle-to-grid services at household level including battery degradation and price uncertainty,” *IET Generation, Transmission & Distribution,* vol. 8, pp. 1007-1016, 2014.

[27] S. Pirouzi, M.A. Latify, and G.R. Yousefi, “Investigation on Reactive Power Support Capability of PEVs in Distribution Network Operation,” *23rd Iranian Conference on Electrical Engineering (ICEE)*, May 2015.

[28] S. Pirouzi, J. Aghaei, M. Shafie-khah, G.J. Osório, J.P.S. Catalão, “Evaluating the security of electrical energy distribution networks in the presence of electric vehicles,” in *Proc. PowerTech Conf, IEEE Manchester*, pp. 1-6, 2017.

[29] S. Pirouzi, J. Aghaei, “Mathematical Modeling of Electric Vehicles Contributions in Voltage Security of Smart Distribution Networks,” SIMULATION: Transactions of the Society for Modeling and Simulation International, (article in press), 2018.

[30] J.F. Benders, “Partitioning procedures for solving mixed-variables programming problems,” *Numer. Math*., vol. 4, no. 1, pp. 238-252, 1962.

[31] S. Pirouzi, and J. Aghaei, T. Niknam, H. Farahmand, and M. Korpås, “Exploring prospective benefits of electric vehicles for optimal energy conditioning in distribution networks,” *Energy,* vol. 157, pp. 679-689, 2018.

[32] S. Pirouzi, J. Aghaei, T. Niknam, H. Farahmand, and M. Korpås, “Proactive Operation of Electric Vehicles in Harmonic Polluted Smart Distribution Networks,” *IET Generation, Transmission and distribution*, vol. 12, pp. 967-975, 2018.

[33] D. Bertsimas, E. Litvinov, X. A. Sun, J. Zhao, and T. Zheng, “Adaptive robust optimization for the security constrained unit commitment problem,” *IEEE Trans. Power Syst*., vol. 28, no. 1, pp. 52-63, Feb. 2013.

[34] A.J. Conejo, E. Castillo, R. Minguez, and R. Garcid-Bertrand, Decomposition Techniques in Mathematical Programming, *Springer,* 2006.

[35] Generalized Algebraic Modeling Systems (GAMS). [Online]. Available: http://www.gams.com.

[36] C. Bucher and G. Andersson, “Generation of domestic load profiles – an adaptive top-down approach,” in Proceedings of PMAPS 2012, Istanbul, Turkey, June 2012.

[37] Nord Pool, https://www.nordpoolgroup.com/historical-market-data/.

[38] M. Malvoni, M.G.D Giorgi, P.M. Congedo, “Data on photovoltaic power forecasting models for Mediterranean climate,” *Data in Brief*, vol. 7, pp. 1639-1642, 2016.